

Type III Seesaw for Neutrino Masses in $U(1)_{B-L}$ Model with Multi-component Dark Matter

Anirban Biswas,^{1,*} Debasish Borah,^{2,†} and Dibyendu Nanda^{2,‡}

¹*School of Physical Sciences, Indian Association for the Cultivation of Science,
2A & 2B Raja S.C. Mullick Road, Kolkata 700032, India*

²*Department of Physics, Indian Institute of Technology Guwahati, Assam 781039, India*

Abstract

We propose a $B - L$ gauged extension of the Standard Model where light neutrino masses arise from type III seesaw mechanism. Unlike the minimal $B - L$ model with three right handed neutrinos having unit lepton number each, the model with three fermion triplets is however not anomaly free. We show that the leftover triangle anomalies can be cancelled by two neutral Dirac fermions having fractional $B - L$ charges, both of which are naturally stable by virtue of a remnant $\mathbb{Z}_2 \times \mathbb{Z}'_2$ symmetry, naturally leading to a two component dark matter scenario without any ad-hoc symmetries. We constrain the model from all relevant phenomenological constraints including dark matter properties. Light neutrino mass and collider prospects are also discussed briefly. Due to additional neutral gauge bosons, the fermion triplets in type III seesaw can have enhanced production cross section in collider experiment.

PACS numbers: 12.60.Fr, 12.60.-i, 14.60.Pq, 14.60.St

*Electronic address: anirban.biswas.sinp@gmail.com

†Electronic address: dborah@iitg.ac.in

‡Electronic address: dibyendu.nanda@iitg.ac.in

I. INTRODUCTION

Origin of light neutrino mass and dark matter (DM) in the universe have been well known mysteries in particle physics for many decades [1]. While two mass squared differences and three mixing angles in the neutrino sector are very well measured [2], evidence suggests that DM gives rise to around 26% of the present universe's energy density. In terms of density parameter Ω_{DM} and $h = \text{Hubble Parameter}/(100 \text{ km s}^{-1}\text{Mpc}^{-1})$, the present DM abundance is conventionally reported as [3]: $\Omega_{\text{DM}}h^2 = 0.120 \pm 0.001$ at 68% CL. Apart from this evidence from cosmology experiments like Planck, there have been plenty of astrophysical evidences accumulated for several decades. Among them, the galaxy cluster observations by Fritz Zwicky [4] in 1933, observations of galaxy rotation curves in 1970's by Rubin and collaborators [5], the observation of the bullet cluster by Chandra observatory [6] along with several galaxy survey experiments which map the distribution of such matter based on their gravitational lensing effects are noteworthy. While all these evidences are based on purely gravitational interactions of dark matter, there have been significant efforts in hunting for other types of interactions, possibly of weak interaction type, at several dark matter direct detection experiments. Such interactions are typical of weakly interacting massive particle (WIMP) dark matter, the most widely studied beyond standard model (BSM) framework for accommodating dark matter. Here a DM candidate typically with electroweak (EW) scale mass and interaction rate similar to EW interactions can give rise to the correct DM relic abundance, a remarkable coincidence often referred to as the *WIMP Miracle* [7]. The very same interactions could also give rise to dark matter nucleon scattering at an observable rate. However, experiments like LUX [8], PandaX-II [9, 10] and XENON1T [11, 12] have so far produced only negative results putting stringent upper limits on DM interactions with the standard model (SM) particles like quarks. Next generation direct detection experiments like LZ [13], XENONnT [14], DARWIN [15] and PandaX-30T [16] are going to probe DM interaction rates very close to the rates at which coherent neutrino-nucleus elastic scattering takes place beyond which it will be extremely difficult to distinguish the neutrino or DM origin of nuclear recoil events. Similar null results have been reported by collider experiments like the large hadron collider (LHC) [17] as well as indirect detection experiments putting stricter upper limits on DM annihilation to standard model (SM) particles [18], specially the charged ones which can finally lead to excess of gamma rays for WIMP type DM. Though

the null results reported by these experiments do not rule out all the parameter space for a single particle WIMP type DM, it may be hinting at a much richer dark sector. Though a single component DM is a very minimal and predictive scenario to begin with, a richer dark sector may in fact be natural given the complicated visible sector. There have been several proposals for multi-component WIMP dark matter during last few years, some of which can be found in [19–35, 35–51]. Going from single component to multi-component DM sector can significantly alter the direct as well as indirect detection rates for DM. Since direct and indirect detection (considering annihilations only, for stable DM) rates of DM are directly proportional to the DM density and DM density squared respectively, multi-component DM models can find larger allowed region of parameter space by appropriate tuning of their relative abundance. In addition to that, such multi-component DM scenarios often give rise to very interesting signatures at direct and indirect detection experiments [23, 32, 37, 52–69].

Similar to the BSM proposals of DM, there have been plenty of ways proposed so far, in order to accommodate light neutrino masses and mixing. While the SM can not generate light neutrino mass at renormalisable level, one can generate a tiny Majorana mass for the neutrinos from the SM Higgs field (H) through the non-renormalisable dimension five Weinberg operator [70] $(LLHH)/\Lambda$, $L \equiv$ lepton doublet, $\Lambda \equiv$ unknown cut-off scale. Dynamical ways to generate such an operator are classified as seesaw mechanism where one or more heavy fields are responsible for tiny light neutrino mass, resulting from the seesaw between electroweak scale and the scale of heavy fields. Popular seesaw models are categorised as type I seesaw [71–74], type II seesaw [75–79], type III seesaw [80] and so on. However, none of these models and their predictions have found any experimental verifications at ongoing experiments like the LHC [81]. In view of this, it is not really outlandish to consider frameworks where DM and neutrino finds common origin opening up the possibility to probe such models at different frontiers with more observables. One popular scenario that is built upon such objectives is the scotogenic framework, originally proposed by Ma [82], where particles odd under an unbroken \mathbb{Z}_2 sector take part in radiative generation of light neutrino masses while the lightest \mathbb{Z}_2 odd particle is the DM candidate. The same formalism was extended to two component DM scenario by the authors of [83]. While multiple copies of \mathbb{Z}_2 symmetries remain ad-hoc in these models, one could find their UV completion with additional gauge symmetries. For example, in a recent work [47], two component fermion DM was proposed as a new anomaly free gauged $B - L$ model, where B and L correspond to baryon and lep-

ton numbers respectively ¹. The neutrino mass in this model originate from just two right handed neutrinos, often referred to as the littlest seesaw (LS) model [86], leading to a vanishing lightest neutrino mass. While TeV scale minimal type I or LS model has limited scope of being verified at experiments like the LHC due to the gauge singlet nature of additional fermions, presence of new gauge symmetries like $U(1)_{B-L}$. Motivated by this, we consider another interesting possibility, within a gauged $B - L$ model, where light neutrino masses arise from a type III seesaw scenario, along with the possibility of a two component fermion DM naturally arising as a possible way to make the model anomaly free. While implementing type I seesaw with three or two right handed neutrinos is a matter of choice (as both are allowed due to the unknown lightest neutrino mass) with the former not requiring any additional fermions (possible DM candidates) for anomaly cancellation, the implementation of type III seesaw in a gauged $B - L$ model inevitably brings in new anomalies due to the non-trivial transformation of fermion triplet fields under the $SU(2)_L$ gauge symmetry of the SM. Out of several possible solutions to the anomaly cancellation conditions, we discuss one possible scenario which naturally leads to a two component fermion DM scenario. The $U(1)_{B-L}$ gauge boson apart from dictating the relic abundance of two component DM, also enhances the production cross section of heavy fermion triplets in proton proton collisions at the LHC due to the on-shell nature of mediating neutral gauge boson. We constrain the model parameters from all relevant constraints from DM sector as well as collider bounds and present the available parameter space.

This paper is organised as follows. In section II, we give an overview of gauged $B - L$ model with different solutions to anomaly conditions including the one we choose to discuss in details in this work. In section III, we discuss our model in details followed by section IV where we mention different existing constraints on model parameters. In section V we discuss in details the coupled Boltzmann equations for two component dark matter in our model followed by section VI where we mention briefly the details of dark matter direct detection. In section VII, we discuss our results related to dark matter relic abundance and constraints on the model parameters from all our requirements and constraints. We briefly mention some interesting LHC signatures of our model in section VIII and then finally

¹ Please see [84, 85] and references therein for general approach to build anomaly free Abelian gauge models with DM.

conclude in section IX.

II. GAUGED $B - L$ SYMMETRY

Gauged $B - L$ symmetric extension of the SM [87–91] is one of the most popular and very well motivated BSM frameworks that has been studied quite well for a long time. Since the SM already has an accidental and global $B - L$ symmetry at renormalisable level, it is very straightforward as well as motivating to uplift it to a gauge symmetry and study the consequences. Compared to an arbitrary Abelian gauge extension of the SM, gauged $B - L$ symmetry emerges as a very natural and minimal possibility as the corresponding charges of all the SM fields under this new symmetry are well known. However, a $U(1)_{B-L}$ gauge symmetry with only the SM fermions is not anomaly free. This is because the triangle anomalies for both $U(1)_{B-L}^3$ and the mixed $U(1)_{B-L} - (\text{gravity})^2$ diagrams are non vanishing. These triangle anomalies for the SM fermion content are given as

$$\begin{aligned}\mathcal{A}_1 [U(1)_{B-L}^3] &= \mathcal{A}_1^{\text{SM}} [U(1)_{B-L}^3] = -3, \\ \mathcal{A}_2 [(\text{gravity})^2 \times U(1)_{B-L}] &= \mathcal{A}_2^{\text{SM}} [(\text{gravity})^2 \times U(1)_{B-L}] = -3.\end{aligned}\tag{1}$$

Remarkably, if three right handed neutrinos are added to the model, they contribute $\mathcal{A}_1^{\text{New}} [U(1)_{B-L}^3] = 3, \mathcal{A}_2^{\text{New}} [(\text{gravity})^2 \times U(1)_{B-L}] = 3$ leading to vanishing total of triangle anomalies. This is the most natural and economical $U(1)_{B-L}$ model where the fermion sector has three right handed neutrinos apart from the usual SM fermions and it has been known for a long time. However, there exist non-minimal ways of constructing anomaly free versions of $U(1)_{B-L}$ model. For example, it has been known for a few years that three right handed neutrinos with exotic $B - L$ charges 5, -4 , -4 can also give rise to vanishing triangle anomalies [92]. It is clear to see how the anomaly cancels, as follows

$$\begin{aligned}\mathcal{A}_1 [U(1)_{B-L}^3] &= \mathcal{A}_1^{\text{SM}} [U(1)_{B-L}^3] + \mathcal{A}_1^{\text{New}} [U(1)_{B-L}^3] = -3 + [-5^3 - (-4)^3 - (-4)^3] = 0, \\ \mathcal{A}_2 [(\text{gravity})^2 \times U(1)_{B-L}] &= \mathcal{A}_2^{\text{SM}} [(\text{gravity})^2 \times U(1)_{B-L}] + \mathcal{A}_2^{\text{New}} [(\text{gravity})^2 \times U(1)_{B-L}], \\ &= -3 + [-5 - (-4) - (-4)] = 0.\end{aligned}\tag{2}$$

This model was also discussed recently in the context of neutrino mass [93, 94] and DM [95–98] by several groups. Another solution to the anomaly cancellation conditions with

irrational $B - L$ charges of new fermions was proposed by the authors of [99] where both DM and neutrino mass can have a common origin through radiative linear seesaw.

Very recently, another anomaly free $U(1)_{B-L}$ framework was proposed where the additional right handed fermions possess more exotic $B - L$ charges namely, $-4/3, -1/3, -2/3, -2/3$ [100]. The triangle anomalies get cancelled as follows.

$$\begin{aligned}\mathcal{A}_1 [U(1)_{B-L}^3] &= \mathcal{A}_1^{\text{SM}} [U(1)_{B-L}^3] + \mathcal{A}_1^{\text{New}} [U(1)_{B-L}^3] \\ &= -3 + [-(-4/3)^3 - (-1/3)^3 - (-2/3)^3 - (-2/3)^3] = 0\end{aligned}$$

$$\begin{aligned}\mathcal{A}_2 [(\text{gravity})^2 \times U(1)_{B-L}] &= \mathcal{A}_2^{\text{SM}} [(\text{gravity})^2 \times U(1)_{B-L}] + \mathcal{A}_2^{\text{New}} [(\text{gravity})^2 \times U(1)_{B-L}] \\ &= -3 + [-(-4/3) - (-1/3) - (-2/3) - (-2/3)] = 0\end{aligned}\quad (3)$$

These four chiral fermions constitute two Dirac fermion mass eigenstates, the lighter of which becomes the DM candidate having either thermal [100] or non-thermal origins [101]. The light neutrino mass in this model had its origin from a variant of type II seesaw mechanism and hence remained disconnected to the anomaly cancellation conditions. In a follow up work by the authors of [102], these fermions with fractional charges were also responsible for generating light neutrino masses at one loop level. One can have even more exotic right handed fermions with $B - L$ charges $-17/3, 6, -10/3$ so that the triangle anomalies cancel as

$$\begin{aligned}\mathcal{A}_1 [U(1)_{B-L}^3] &= \mathcal{A}_1^{\text{SM}} [U(1)_{B-L}^3] + \mathcal{A}_1^{\text{New}} [U(1)_{B-L}^3] , \\ &= -3 + [-(-17/3)^3 - (6)^3 - (-10/3)^3] = 0 ,\end{aligned}$$

$$\begin{aligned}\mathcal{A}_2 [(\text{gravity})^2 \times U(1)_{B-L}] &= \mathcal{A}_2^{\text{SM}} [(\text{gravity})^2 \times U(1)_{B-L}] + \mathcal{A}_2^{\text{New}} [(\text{gravity})^2 \times U(1)_{B-L}] , \\ &= -3 + [-(-17/3) - (6) - (-10/3)] = 0 .\end{aligned}\quad (4)$$

In the recent work on $U(1)_{B-L}$ gauge symmetry with two component DM [47], the authors considered two right handed neutrinos with $B - L$ number -1 each so that the model still remains anomalous. The remaining anomalies were cancelled by four chiral fermions with fractional $B - L$ charges leading to two Dirac fermion mass eigenstates both of which are stable and hence DM candidates.

To implement type III seesaw in $U(1)_{B-L}$ model, we consider two copies ($n_\Sigma = 2$) of fermion triplets $\Sigma_{Ri} (i = 1, 2)$ into the model having quantum numbers $(1, 3, 0, -1)$ under

$SU(3)_c, SU(2)_L, U(1)_Y$ and $U(1)_{B-L}$ gauge groups respectively. Note that, two copies are enough to satisfy the light neutrino data, as in LS models. The non-vanishing anomalies are

$$[SU(2)_L]^2 U(1)_{B-L} = 2n_\Sigma = 4, \quad [U(1)_{B-L}]^3 = -3 + 3n_\Sigma = 3, \quad [U(1)_{B-L}] = -3 + 3n_\Sigma = 3. \quad (5)$$

Note that the first anomaly is arising only due to the $SU(2)_L$ transformation of newly introduced fermions and was absent in the minimal $B - L$ extension of SM. Obviously, the first anomaly can be cancelled only by introducing an additional field which has non-trivial transformation under both $SU(2)_L$ and $U(1)_{B-L}$. We introduce such additional fields with a goal to keep our setup minimal and connected to the origin of light neutrino mass. Introducing a quintuplet $\Psi(1, 4, 0, n_1)$, the first anomaly becomes

$$[SU(2)_L]^2 U(1)_{B-L} = 2n_\Sigma - 5n_1$$

which can vanish if $n_1 = 2n_\Sigma/5 = 4/5$. The other anomalies can be cancelled by introducing additional fields which do not contribute to the first anomaly and hence $SU(2)_L$ singlets. The remaining anomalies are

$$[U(1)_{B-L}]^3 = -3 + 3n_\Sigma - 4n_1^3 = \frac{119}{125}, \quad [U(1)_{B-L}] = -3 + 3n_\Sigma - 4n_1 = -\frac{1}{5}. \quad (6)$$

These remaining anomalies can be cancelled by introducing three $SU(2)_L$ singlet chiral fermions

$$N_{1L}(1, 1, 0, -\frac{7}{5}), N_{2L}(1, 1, 0, \frac{2}{5}), N_{3L}(1, 1, 0, \frac{6}{5}). \quad (7)$$

This can be seen as follows

$$[U(1)_{B-L}]^3 = -3 + 3n_\Sigma - 4n_1^3 - \left(\frac{7}{5}\right)^3 + \left(\frac{2}{5}\right)^3 + \left(\frac{6}{5}\right)^3 = \frac{119}{125} - \frac{119}{125} = 0,$$

$$[U(1)_{B-L}] = -3 + 3n_\Sigma - 4n_1 - \frac{7}{5} + \frac{2}{5} + \frac{6}{5} = -\frac{1}{5} + \frac{1}{5} = 0.$$

Since the quintuplet and the other singlet fermions have no role to play in generating light neutrino mass, we do not pursue this possibility further.

We can have three fermion triplets: two of them having $B - L$ charge -1 and the third having exotic charge n_1 . We will check if the third fermion can have any possible role in

generating light neutrino masses. In such a case, there arises a possibility to get vanishing $[SU(2)_L]^2 U(1)_{B-L}$ anomaly. In this case,

$$[SU(2)_L]^2 U(1)_{B-L} = 2n_\Sigma - 2n_1$$

which can vanish if $n_1 = n_\Sigma = 2$. The other anomalies can be cancelled by introducing additional fields which do not contribute to the first anomaly and hence $SU(2)_L$ singlets. The remaining anomalies are

$$[U(1)_{B-L}]^3 = -3 + 3n_\Sigma - 3n_1^3 = -21, \quad [U(1)_{B-L}] = -3 + 3n_\Sigma - 3n_1 = -3. \quad (8)$$

We now consider different possible solutions to these anomalies one by one.

Solution 2:

The remaining anomalies mentioned above can be cancelled by introducing four $SU(2)_L$ singlet chiral fermions

$$N_{1R}(1, 1, 0, 2), N_{2R}(1, 1, 0, -1), N_{3R}(1, 1, 0, -1), N_{4R}(1, 1, 0, -3). \quad (9)$$

This can be seen as follows

$$[U(1)_{B-L}]^3 = -3 + 3n_\Sigma - 3n_1^3 - (2)^3 - 2(-1)^3 - (-3)^3 = -21 + 21 = 0,$$

$$[U(1)_{B-L}] = -3 + 3n_\Sigma - 3n_1 - 2 + 1 + 1 + 3 = -3 + 3 = 0.$$

However, this solution is not very motivating owing to the existence of singlet fermions having $B-L$ charge -1 , which will give type I seesaw contribution to light neutrino masses, already discussed by several earlier works.

Solution 3:

The remaining anomalies can also be cancelled by the following fermions with fractional $B-L$ charges:

$$N_{1R}(1, 1, 0, \frac{2}{3}), N_{2R}(1, 1, 0, \frac{1}{3}), N_{3R}(1, 1, 0, -\frac{4}{3}), N_{4R}(1, 1, 0, -\frac{8}{3}). \quad (10)$$

In order to have non-zero masses for all new fermions and sticking to minimal scalar contents having integer $B-L$ charges, we find that there can be one stable dark matter candidate, in terms of one of the singlet fermions. Since single component dark matter in such models have already been discussed in several works, we do not pursue this possibility further.

Solution 4:

The most interesting possibility is the solution

$$N_{1R}(1, 1, 0, \frac{7}{5}), N_{2R}(1, 1, 0, -\frac{2}{5}), N_{3R}(1, 1, 0, -\frac{6}{5}), N_{4R}(1, 1, 0, -\frac{14}{5}). \quad (11)$$

which can also be recast as

$$N_{1L}(1, 1, 0, -\frac{7}{5}), N_{1R}(1, 1, 0, -\frac{2}{5}), N_{2L}(1, 1, 0, \frac{6}{5}), N_{2R}(1, 1, 0, -\frac{14}{5}). \quad (12)$$

We can construct two Dirac fermions from these four chiral ones, just by introducing two singlet scalars ϕ_1, ϕ_2 having $B - L$ charges 1, 4 respectively. The corresponding mass terms will be

$$Y_1 \overline{N_{1L}} N_{1R} \phi_1^\dagger + Y_2 \overline{N_{2L}} N_{2R} \phi_2 + \text{h.c.}$$

Another scalar singlet having $B - L$ charge 2 is also required in order to give mass to the fermion triplets $\Sigma_{1,2}$. The third fermion triplet acquires mass and also mixes with the other two fermion triplets by virtue of its couplings to the scalars ϕ_1, ϕ_2 . Although the third fermion triplet is not stable due to its mixing with the first two, the two Dirac fermions constructed above can be separately stable and hence give rise to multi-component dark matter. Also, the third fermion triplet, through its mixing with the first two, can contribute to the light neutrino mass matrix as we discuss in details in upcoming sections. Due to these interesting possibilities, we pursue this scenario in our work.

III. THE MODEL

In this section we have discussed our model elaborately. As mentioned earlier, in this work our prime motivation is to have a multicomponent dark matter scenario where both dark matter candidates are stable by virtue of a single symmetry group. Additionally, we want to address neutrino mass generation as well. Keeping these two things in our mind, we have extended the SM in all three sectors namely the gauge sector, the fermionic sector and the scalar sector. In the gauge sector, we have demanded an additional local $U(1)_{B-L}$ gauge invariance where B and L are denoting baryon and lepton numbers respectively of a particular field. This introduces anomalies (both axial vector and gauge-gravitational anomalies) in the theory which can only be evaded by the inclusion of additional fermionic degrees of freedom. This has elaborately been discussed in the previous section. We have

Particles	$SU(3)_c \times SU(2)_L \times U(1)_Y \times U(1)_{B-L}$
$q_L = \begin{pmatrix} u_L \\ d_L \end{pmatrix}$	$(3, 2, \frac{1}{6}, \frac{1}{3})$
u_R	$(3, 1, \frac{2}{3}, \frac{1}{3})$
d_R	$(3, 1, -\frac{1}{3}, \frac{1}{3})$
$\ell_L = \begin{pmatrix} \nu_L \\ e_L \end{pmatrix}$	$(1, 2, -\frac{1}{2}, -1)$
e_R	$(1, 1, -1, -1)$
Σ_{R1}	$(1, 3, 0, -1)$
Σ_{R2}	$(1, 3, 0, -1)$
Σ_{R3}	$(1, 3, 0, 2)$
N_{1L}	$(1, 1, 0, -\frac{7}{5})$
N_{1R}	$(1, 1, 0, -\frac{2}{5})$
N_{2L}	$(1, 1, 0, \frac{6}{5})$
N_{2R}	$(1, 1, 0, -\frac{14}{5})$

TABLE I: Fermionic fields of the present Model including the SM fermions.

seen that for the case of three additional $SU(2)_L$ triplet fermions Σ_{Ri} , $i = 1$ to 3 , two of which with $B - L$ charge -1 are necessary to generate neutrino masses via Type-III seesaw mechanism and the rest having $B - L$ charge 2 is solely required to cancel $[SU(2)_L]^2 U(1)_{B-L}$ anomaly. We further need four SM gauge singlet chiral fermions with fractional $B - L$ charges to cancel both $U(1)_{B-L}^3$ and $(\text{gravity})^2 U(1)_{B-L}$ anomalies. Moreover, at least three scalar fields ϕ_i ($i = 1$ to 3) are also necessary to give masses to all new fermions in the broken phase of the $U(1)_{B-L}$ symmetry. We have properly adjusted $B - L$ charges of these ϕ_i s such that only the Dirac mass terms among these singlet fermions are possible and more importantly the Dirac mass matrix is diagonal. This results in two physical Dirac fermions out of these four chiral fermions which are simultaneously stable and thus both can be viable dark matter candidates. In Tables I and II, we have listed all fermions as well as scalar fields (including the SM ones) of the present model and their charges under the $SU(3)_c \times SU(2)_L \times U(1)_Y \times U(1)_{B-L}$ symmetry.

Particles	$SU(3)_c \times SU(2)_L \times U(1)_Y \times U(1)_{B-L}$
$H = \begin{pmatrix} H^+ \\ H^0 \end{pmatrix}$	$(1, 2, \frac{1}{2}, 0)$
ϕ_1	$(1, 1, 0, 1)$
ϕ_2	$(1, 1, 0, 4)$
ϕ_3	$(1, 1, 0, 2)$

TABLE II: Scalar fields and their corresponding charges under all the symmetry groups.

The Lagrangian of our present model invariant under the full symmetry group is given by

$$\mathcal{L} = \mathcal{L}_{SM} - \frac{1}{4} B'_{\alpha\beta} B'^{\alpha\beta} + \mathcal{L}_{scalar} + \mathcal{L}_{fermion} . \quad (13)$$

Here, \mathcal{L}_{SM} denotes the SM Lagrangian involving quarks, gluons, charged leptons, left handed neutrinos and electroweak gauge bosons. The second term is the kinetic term of $B-L$ gauge boson (Z_{BL}) expressed in terms of field strength tensor $B'^{\alpha\beta} = \partial^\alpha Z_{BL}^\beta - \partial^\beta Z_{BL}^\alpha$. From Table II, we have already understood that our model has a very rich scalar sector and the gauge invariant interactions among the scalar fields are described by \mathcal{L}_{scalar} which contains following terms,

$$\begin{aligned} \mathcal{L}_{scalar} = & (D_{H\mu} H)^\dagger (D_H^\mu H) + \sum_{i=1}^3 \left(D_{\phi_i\mu} \phi_i \right)^\dagger (D_{\phi_i}^\mu \phi_i) - \left[-\mu_H^2 (H^\dagger H) + \lambda_H (H^\dagger H)^2 \right. \\ & + \sum_{i=1}^3 \left(-\mu_{\phi_i}^2 (\phi_i^\dagger \phi_i) + \lambda_{\phi_i} (\phi_i^\dagger \phi_i)^2 \right) + \sum_{i,j=1(i \neq j)}^3 \lambda_{\phi_i \phi_j} (\phi_i^\dagger \phi_i) (\phi_j^\dagger \phi_j) \\ & \left. + \sum_{i=1}^3 \lambda_{H\phi_i} (H^\dagger H) (\phi_i^\dagger \phi_i) + \left(\beta \phi_1 \phi_1 \phi_3 \phi_2^\dagger + \delta \phi_1 \phi_1 \phi_3^\dagger + \zeta \phi_3 \phi_3 \phi_2^\dagger + h.c. \right) \right] , \quad (14) \end{aligned}$$

where covariant derivatives for the Higgs doublet H and singlet scalars ϕ_i s are defined as

$$\begin{aligned} D_{H\mu} H &= \left(\partial_\mu + i \frac{g}{2} \sigma_a W_\mu^a + i \frac{g'}{2} B_\mu \right) H , \\ D_{\phi_\mu} \phi_i &= \left(\partial_\mu + i g_{BL} n_{\phi_i} Z_{BL\mu} \right) \phi_i . \end{aligned} \quad (15)$$

The quantity $D_{H\mu}$ is the usual covariant derivative of the SM Higgs doublet with g and g' are gauge couplings of $SU(2)_L$ and $U(1)_Y$ respectively and the corresponding gauge bosons

are denoted by W_μ^a ($a = 1, 3$) and B_μ . The covariant derivative of H does not include $B - L$ gauge boson Z_{BL} as the corresponding gauge charge of H is zero. On the other hand, being a SM gauge singlet, covariant derivative of ϕ_i only contains Z_{B-L} with n_{ϕ_i} is the respective $B - L$ charge of ϕ_i and g_{BL} is the new gauge coupling. After breaking of both $B - L$ symmetry and electroweak symmetry by the VEVs of H and ϕ_i s, the doublet and all three singlets are given by

$$H = \begin{pmatrix} H^+ \\ \frac{h' + v + iz}{\sqrt{2}} \end{pmatrix}, \quad \phi_i = \frac{s'_i + u_i + A'_i}{\sqrt{2}} \quad (i = 1, 2, 3), \quad (16)$$

where v and u_i s ($i = 1, 2, 3$) are VEVs of H and ϕ_i s respectively. For calculational simplicity we have assumed all three VEVs of singlet scalars are equal i.e. $u_1 = u_2 = u_3 = u$. Therefore, substituting Eq. (16) in Eq. (14) we have a 4×4 mixing matrix for the real scalar fields in the basis $\frac{1}{\sqrt{2}}(h' \ s'_1 \ s'_2 \ s'_3)^T$ which has the following form,

$$\mathcal{M}_{rs} = \begin{pmatrix} 2\lambda_H v^2 & \lambda_{H\phi_1} u v & \lambda_{H\phi_2} u v & \lambda_{H\phi_3} u v \\ \lambda_{H\phi_1} u v & 2\lambda_{\phi_1} u^2 & u^2(\beta + \lambda_{\phi_1\phi_2}) & u(\sqrt{2}\delta + u(\beta + \lambda_{\phi_1\phi_3})) \\ \lambda_{H\phi_2} u v & u^2(\beta + \lambda_{\phi_1\phi_2}) & -\frac{1}{2}u(\sqrt{2}\zeta + u(\beta - 4\lambda_{\phi_2})) & \frac{1}{2}u(2\sqrt{2}\zeta + u(\beta + 2\lambda_{\phi_2\phi_3})) \\ \lambda_{H\phi_3} u v & u(\sqrt{2}\delta + u(\beta + \lambda_{\phi_1\phi_3})) & \frac{1}{2}u(2\sqrt{2}\zeta + u(\beta + 2\lambda_{\phi_2\phi_3})) & -\frac{1}{2}u(\sqrt{2}\delta + u(\beta - 4\lambda_{\phi_3})) \end{pmatrix}. \quad (17)$$

The physical scalars (h, s_1, s_2, s_3) are obtained by diagonalising the above real symmetric mass matrix and they are related by an orthogonal transformation to the unphysical scalars (i.e. the basis state before diagonalisation) as

$$\begin{pmatrix} h \\ s_1 \\ s_2 \\ s_3 \end{pmatrix} = \mathcal{O}^T \begin{pmatrix} h' \\ s'_1 \\ s'_2 \\ s'_3 \end{pmatrix}, \quad (18)$$

where \mathcal{O} is a 4×4 orthogonal matrix which makes \mathcal{M}_{rs} diagonal i.e. $\mathcal{O}^T \mathcal{M}_{rs} \mathcal{O} \Rightarrow$ a diagonal matrix containing all the masses of four physical scalars as diagonal elements. In Appendix A, we have expressed all the elements of \mathcal{O} matrix in terms of four mixing angles (assuming mixing among the three singlet scalars are identical). Additionally, for simplicity we also set $\beta = 0$, ² and $\zeta = \delta$ in Eq. (14).

² β is the coupling of quartic interaction among all four singlet scalars which has less significant impact in

On the other hand, in our model we have four pseudo scalars as well, which are z , A'_1 , A'_2 and A'_3 (see Eq. (16)). Out of these four pseudo scalars, z does not mix with others and becomes the Goldstone boson corresponding to the SM Z boson after EWSB. However, the pseudo scalars of complex singlet ϕ_i s mix among each other when $B - L$ symmetry is broken by the VEVs of ϕ_i s. Therefore, unlike the case of real scalars, here we have a 3×3 mixing matrix in the basis $\frac{1}{\sqrt{2}}(A'_1 \ A'_2 \ A'_3)^T$ which is written below,

$$\mathcal{M}_{ps} = \begin{pmatrix} -2u(u\beta + \sqrt{2}\delta) & u^2\beta & u(-u\beta + \sqrt{2}\delta) \\ u^2\beta & -\frac{u}{2}(u\beta + \sqrt{2}\zeta) & \frac{u}{2}(u\beta + 2\sqrt{2}\zeta) \\ u(-u\beta + \sqrt{2}\delta) & \frac{u}{2}(u\beta + 2\sqrt{2}\zeta) & -\frac{u}{2}(u\beta + \sqrt{2}(\delta + 4\zeta)) \end{pmatrix}. \quad (19)$$

After diagonalising, this matrix we get two physical pseudo scalars A_2 , A_3 and a massless Goldstone boson A_1 corresponding to the extra neutral gauge boson Z_{BL} . This can easily be checked as the pseudo scalar mass matrix has a null determinant. The eigenvalues of the pseudo scalar mass matrix for $\zeta = \delta$, $\beta = 0$ are³

$$\begin{aligned} m_{A_2}^2 &= -\frac{3\zeta u}{\sqrt{2}}, \\ m_{A_3}^2 &= -\frac{7\zeta u}{\sqrt{2}}, \end{aligned} \quad (20)$$

where ζ must be less than zero to ensure m_{A_2} and m_{A_3} are real. Further, the physical CP-odd scalars (A_i s) and the Goldstone boson A_1 are related to the unphysical basis states (A'_1 , A'_2 , A'_3) as follows

$$\begin{pmatrix} A_1 \\ A_2 \\ A_3 \end{pmatrix} = \begin{pmatrix} \frac{1}{\sqrt{21}} & \frac{4}{\sqrt{21}} & \frac{2}{\sqrt{21}} \\ \frac{2}{\sqrt{3}} & -\frac{1}{\sqrt{6}} & \frac{1}{\sqrt{6}} \\ -\frac{2}{\sqrt{7}} & \frac{1}{\sqrt{14}} & \frac{3}{\sqrt{14}} \end{pmatrix} \begin{pmatrix} A'_1 \\ A'_2 \\ A'_3 \end{pmatrix}. \quad (21)$$

Moreover, the neutral gauge boson Z_{BL} becomes massive after the breaking of $U(1)_{B-L}$ and the corresponding mass term of Z_{B-L} is given by

$$\begin{aligned} M_{Z_{BL}} &= g_{BL} \sqrt{\left(\sum_{i=1}^3 n_{\phi_i}^2 u_i^2 \right)}, \\ &= \sqrt{21} g_{BL} u. \end{aligned} \quad (22)$$

dark matter phenomenology compared to other cubic scalar interaction terms like $\delta \phi_1 \phi_1 \phi_3^\dagger$ and $\zeta \phi_3 \phi_3 \phi_2^\dagger$.

³ Eigenvalues of \mathcal{M}_{ps} for $\zeta \neq \delta \neq \beta$ are given in Appendix B.

Now, let us concentrate on the fermionic sector of the present model. Here, in addition to the usual SM fermions, we have four gauge singlet fermions and three $SU(2)_L$ triplet fermions. All these new fermions have appropriate $B - L$ charges. In Eq. (13), \mathcal{L}_f is the Lagrangian for these newly added fermionic fields and it is composed of two parts as

$$\mathcal{L}_f = \mathcal{L}_{Singlet} + \mathcal{L}_{Triplet}, \quad (23)$$

where, the Lagrangian for the singlet fields are given below

$$\mathcal{L}_{Singlet} = i \sum_{\kappa=1}^2 [N_{\kappa L} \not{D}(Q_{\kappa}^L) N_{\kappa L} + N_{\kappa R} \not{D}(Q_{\kappa}^R) N_{\kappa R}] - \left(\mathcal{Y}_1 \overline{N_{1L}} N_{1R} \phi_1^\dagger + \mathcal{Y}_2 \overline{N_{2L}} N_{2R} \phi_2 + \text{h.c.} \right). \quad (24)$$

In the above \mathcal{Y}_i ($i = 1, 2$) are the dimensionless Yukawa couplings and the covariant derivative is defined as

$$\not{D}(Q_{\kappa}^{L(R)}) N_{\kappa L(R)} = \gamma^\mu (\partial_\mu + i g_{BL} Q_{\kappa}^{L(R)} Z_{BL\mu}) N_{\kappa L(R)}, \quad (25)$$

where $Q_{\kappa}^{L(R)}$ is the corresponding $B - L$ charge of $N_{\kappa L(R)}$ which is listed in Table I. As mentioned earlier, due to special choice of $B - L$ charges of scalar fields ϕ_1 , ϕ_2 and ϕ_3 , the Yukawa interactions in Eq. (24) are exactly diagonal in the basis $\xi_1 = N_{1L} + N_{1R}$ and $\xi_2 = N_{2L} + N_{2R}$. In this basis above Lagrangian can be rewritten as,

$$\begin{aligned} \mathcal{L}_{Singlet} = & i \overline{\xi_1} \not{\partial} \xi_1 + i \overline{\xi_2} \not{\partial} \xi_2 - g_{BL} \left(-\frac{7}{5} \right) \overline{\xi_1} \not{Z}_{BL} P_L \xi_1 - g_{BL} \left(\frac{6}{5} \right) \overline{\xi_2} \not{Z}_{BL} P_L \xi_2 \\ & - g_{BL} \left(-\frac{2}{5} \right) \overline{\xi_1} \not{Z}_{BL} P_R \xi_1 - g_{BL} \left(-\frac{14}{5} \right) \overline{\xi_2} \not{Z}_{BL} P_R \xi_2 - \mathcal{Y}_1 \overline{\xi_1} P_R \xi_1 \phi_1^\dagger \\ & - \mathcal{Y}_2 \overline{\xi_2} P_R \xi_2 \phi_2 - \mathcal{Y}_1 \overline{\xi_1} P_L \xi_1 \phi_1 - \mathcal{Y}_2 \overline{\xi_2} P_L \xi_2 \phi_2^\dagger, \end{aligned}$$

which can be further simplified as

$$\begin{aligned} = & i \overline{\xi_1} \not{\partial} \xi_1 + i \overline{\xi_2} \not{\partial} \xi_2 + \frac{g_{BL}}{10} \overline{\xi_1} \not{Z}_{BL} (9 - 5\gamma_5) \xi_1 + \frac{2g_{BL}}{5} \overline{\xi_2} \not{Z}_{BL} (2 + 5\gamma_5) \xi_2 \\ & - \mathcal{Y}_1 \overline{\xi_1} P_R \xi_1 \phi_1^\dagger - \mathcal{Y}_2 \overline{\xi_2} P_R \xi_2 \phi_2 - \mathcal{Y}_1 \overline{\xi_1} P_L \xi_1 \phi_1 - \mathcal{Y}_2 \overline{\xi_2} P_L \xi_2 \phi_2^\dagger, \end{aligned} \quad (26)$$

where $P_{L,R} = \frac{1 \pm \gamma_5}{2}$, left and right chiral projection operators. Besides, in the above we have assumed the Yukawa couplings \mathcal{Y}_i s are real. Therefore, from the above Lagrangian one can easily notice that both ξ_1 and ξ_2 are decoupled from each other and thus can be stable simultaneously. Hence, they naturally form a two component dark matter system

stabilises by the $B - L$ symmetry only ⁴. On the other hand, $SU(2)_L \times U(1)_{B-L}$ ⁵ invariant Lagrangian for the triplet fields are given by,

$$\begin{aligned} \mathcal{L}_{\text{Triplet}} = & \frac{i}{2} \sum_{k=1}^3 \left(\text{Tr} [\overline{\Sigma_{kR}} \not{D} \Sigma_{kR}] + \text{Tr} [\overline{\Sigma_{kR}^c} \not{D}' \Sigma_{kR}^c] \right) - \frac{1}{2} \left(\text{Tr} [\overline{\Sigma_{1R}^c} \sqrt{2} Y_{\Sigma_1 \phi_3} \Sigma_{1R}] \phi_3 \right. \\ & + \text{Tr} [\overline{\Sigma_{2R}^c} \sqrt{2} Y_{\Sigma_2 \phi_3} \Sigma_{2R}] \phi_3 + \text{Tr} [\overline{\Sigma_{3R}^c} \sqrt{2} Y_{\Sigma_3 \phi_2} \Sigma_{3R}] \phi_2^\dagger + h.c. \Big) - \frac{1}{2} \left\{ \left(\text{Tr} [\overline{\Sigma_{1R}^c} \sqrt{2} Y_{\Sigma_{13} \phi_1} \Sigma_{3R}] \right. \right. \\ & + \text{Tr} [\overline{\Sigma_{3R}^c} \sqrt{2} Y_{\Sigma_{13} \phi_1} \Sigma_{1R}] \Big) \phi_1^\dagger + \left(\text{Tr} [\overline{\Sigma_{2R}^c} \sqrt{2} Y_{\Sigma_{23} \phi_1} \Sigma_{3R}] + \text{Tr} [\overline{\Sigma_{3R}^c} \sqrt{2} Y_{\Sigma_{23} \phi_1} \Sigma_{2R}] \right) \phi_1^\dagger \\ & + \left. \left(\text{Tr} [\overline{\Sigma_{1R}^c} \sqrt{2} Y_{\Sigma_{12} \phi_3} \Sigma_{2R}] + \text{Tr} [\overline{\Sigma_{2R}^c} \sqrt{2} Y_{\Sigma_{12} \phi_3} \Sigma_{1R}] \right) \phi_3 + h.c. \right\}, \end{aligned} \quad (27)$$

where, we consider fermion triplets Σ_{kR} and its CP conjugate Σ_{kR}^c in 2×2 representation as

$$\Sigma_{kR} = \begin{pmatrix} \Sigma_{kR}^0 / \sqrt{2} & \Sigma_{kR}^+ \\ \Sigma_{kR}^- & -\Sigma_{kR}^0 / \sqrt{2} \end{pmatrix}, \quad \Sigma_{kR}^c = \mathbb{C} \overline{\Sigma_{kR}}^T = \begin{pmatrix} \Sigma_{kR}^{0c} / \sqrt{2} & \Sigma_{kR}^{-c} \\ \Sigma_{kR}^{+c} & -\Sigma_{kR}^{0c} / \sqrt{2} \end{pmatrix}, \quad (28)$$

where \mathbb{C} is the charge conjugation matrix. The covariant derivatives used in the kinetic terms of Σ_{kR} and Σ_{kR}^c can be defined as

$$D_\mu^{(\prime)} \Sigma_{kR}^{(c)} = \left(\partial_\mu + i \frac{g}{2} \sigma_a W_\mu^a + (-) i g_{BL} n_\Sigma^k Z_{BL\mu} \right) \Sigma_{kR}^{(c)}, \quad (29)$$

where n_Σ^k is the $B - L$ charge of Σ_{kR} and there is a sign flip as the $B - L$ charges of Σ_{kR} and its CP conjugate are equal but opposite in sign. Now, we define $\psi_k^0 = \Sigma_{kR}^0 + \Sigma_{kR}^{0c}$, a Majorana fermion and a Dirac fermion $\psi_k^- = \Sigma_{kR}^- + \Sigma_{kR}^{+c}$. Following [103], we have written

⁴ Actually, we consider the $B - L$ charges of ϕ_1 , ϕ_2 and ϕ_3 in such a way that $U(1)_{B-L}$ breaks into a $\mathbb{Z}_2 \times \mathbb{Z}_2'$ symmetry where ξ_1 and ξ_2 have following charges $(-, +)$ and $(+, -)$ under the $\mathbb{Z}_2 \times \mathbb{Z}_2'$ symmetry respectively.

⁵ Triplet fermion fields have no colour charge and hypercharge.

the triplet Lagrangian in terms of ψ_k^0 and ψ_k^- as

$$\begin{aligned}
\mathcal{L}_{Triplet} = & \sum_{k=1}^3 \left\{ \frac{i}{2} \overline{\psi_k^0} \not{\partial} \psi_k^0 + i \overline{\psi_k^-} \not{\partial} \psi_k^- - g \left(\overline{\psi_k^-} W^- \psi_k^0 + h.c. \right) + g \sin \theta_W \overline{\psi_k^-} A \psi_k^- \right. \\
& + g \cos \theta_W \overline{\psi_k^-} \not{Z} \psi_k^- - g_{BL} n_\Sigma^k \left(\frac{1}{2} \overline{\psi_k^0} \not{Z}_{BL} \gamma_5 \psi_k^0 + \overline{\psi_k^-} \not{Z}_{BL} \gamma_5 \psi_k^- \right) \Big\} \\
& - \sum_{i=1}^2 Y_{\Sigma_i \phi_3} \left\{ \left(\frac{1}{2} \overline{\psi_i^0} \psi_i^0 + \overline{\psi_i^-} \psi_i^- \right) s'_3 + i \left(\frac{1}{2} \overline{\psi_i^0} \gamma_5 \psi_i^0 + \overline{\psi_i^-} \gamma_5 \psi_i^- \right) A'_3 \right\} \\
& - Y_{\Sigma_3 \phi_2} \left\{ \left(\frac{1}{2} \overline{\psi_3^0} \psi_3^0 + \overline{\psi_3^-} \psi_3^- \right) s'_2 - i \left(\frac{1}{2} \overline{\psi_3^0} \gamma_5 \psi_3^0 + \overline{\psi_3^-} \gamma_5 \psi_3^- \right) A'_2 \right\} \\
& - Y_{\Sigma_{13} \phi_1} \left\{ \left(\frac{1}{2} \overline{\psi_1^0} \psi_3^0 + \overline{\psi_1^-} \psi_3^- \right) s'_1 - i \left(\frac{1}{2} \overline{\psi_1^0} \gamma_5 \psi_3^0 + \overline{\psi_1^-} \gamma_5 \psi_3^- \right) A'_1 + h.c. \right\} \\
& - Y_{\Sigma_{23} \phi_1} \left\{ \left(\frac{1}{2} \overline{\psi_2^0} \psi_3^0 + \overline{\psi_2^-} \psi_3^- \right) s'_1 - i \left(\frac{1}{2} \overline{\psi_2^0} \gamma_5 \psi_3^0 + \overline{\psi_2^-} \gamma_5 \psi_3^- \right) A'_1 + h.c. \right\} \\
& - Y_{\Sigma_{12} \phi_3} \left\{ \left(\frac{1}{2} \overline{\psi_1^0} \psi_2^0 + \overline{\psi_1^-} \psi_2^- \right) s'_3 + i \left(\frac{1}{2} \overline{\psi_1^0} \gamma_5 \psi_2^0 + \overline{\psi_1^-} \gamma_5 \psi_2^- \right) A'_3 + h.c. \right\} , \quad (30)
\end{aligned}$$

$\theta_W = \tan^{-1} \frac{g'}{g}$ is the weak mixing angle (Weinberg angle). The last two terms of the above Lagrangian introduce off-diagonal elements in the mass matrices of both ψ_k^0 and ψ_k^- (k runs from 1 to 3) when s'_1 gets a nonzero VEV. As a result, one needs to diagonalise both the mass matrices using bi-unitary transformations in order to get the physical fermionic states. However, in this work we have not considered this. We have worked in a limit when $Y_{\Sigma_1 \phi_3}$, $Y_{\Sigma_2 \phi_3}$ and $Y_{\Sigma_3 \phi_2} \gg Y_{\Sigma_{13} \phi_1}$ and $Y_{\Sigma_{23} \phi_1}$, so that mass matrices of both charged and neutral fermions are effectively diagonal and thus, there is no need for basis transformation. Here, two triplet fermions having $B - L$ charge -1 will play crucial role in generating observed neutrino masses and mixings via Type-III seesaw mechanism. The Yukawa Lagrangian involving the leptons is given by

$$\mathcal{L}_{Yukawa} \supset \left(\sum_{\alpha=1,2,3, \beta=1,2} \sqrt{2} y_\Sigma^{\alpha\beta} \overline{l_{\alpha L}} \Sigma_{\beta R} \tilde{\Phi} + h.c. \right) \quad (31)$$

The light neutrino mass matrix is generated from the type III seesaw mechanism as

$$M_\nu = -M_D M_R^{-1} M_D^T \quad (32)$$

where the Dirac neutrino mass matrix M_D and neutral triplet fermion mass matrix M_R are

given by

$$M_D = \begin{pmatrix} y_\Sigma^{11} v & y_\Sigma^{12} v & 0 \\ y_\Sigma^{21} v & y_\Sigma^{22} v & 0 \\ y_\Sigma^{31} v & y_\Sigma^{32} v & 0 \end{pmatrix}, \quad M_R = \begin{pmatrix} Y_{\Sigma_1 \phi_3} u_3 & Y_{\Sigma_{12} \phi_3} u_3 & Y_{\Sigma_{13} \phi_1} u_1 \\ Y_{\Sigma_{12} \phi_3} u_3 & Y_{\Sigma_2 \phi_3} u_3 & Y_{\Sigma_{23} \phi_1} u_1 \\ Y_{\Sigma_{13} \phi_1} u_1 & Y_{\Sigma_{23} \phi_1} u_1 & Y_{\Sigma_3 \phi_2} u_2 \end{pmatrix}. \quad (33)$$

Diagonalisation of the light neutrino mass matrix using the above forms of M_D, M_R gives one vanishing mass eigenvalue. This is same as the prediction of the recent work [47] as well as the littlest seesaw model [86] mentioned earlier. If we simplify our neutral fermion triplet mass matrix M_R by incorporating the smallness on off-diagonal Yukawa couplings mentioned earlier $Y_{\Sigma_1 \phi_3}, Y_{\Sigma_2 \phi_3}, Y_{\Sigma_3 \phi_2} \gg Y_{\Sigma_{13} \phi_1}, Y_{\Sigma_{23} \phi_1}, Y_{\Sigma_{12} \phi_3}$ and equality of singlet VEVs, we can approximate M_R to be a diagonal matrix leading to a relatively simple light neutrino mass matrix given as

$$M_\nu = -\frac{v^2}{u} \begin{pmatrix} \frac{(y_\Sigma^{11})^2}{Y_{\Sigma_1 \phi_3}} + \frac{(y_\Sigma^{12})^2}{Y_{\Sigma_2 \phi_3}} & \frac{y_\Sigma^{11} y_\Sigma^{21}}{Y_{\Sigma_1 \phi_3}} + \frac{y_\Sigma^{12} y_\Sigma^{22}}{Y_{\Sigma_2 \phi_3}} & \frac{y_\Sigma^{11} y_\Sigma^{31}}{Y_{\Sigma_1 \phi_3}} + \frac{y_\Sigma^{12} y_\Sigma^{32}}{Y_{\Sigma_2 \phi_3}} \\ \frac{y_\Sigma^{11} y_\Sigma^{21}}{Y_{\Sigma_1 \phi_3}} + \frac{y_\Sigma^{12} y_\Sigma^{22}}{Y_{\Sigma_2 \phi_3}} & \frac{(y_\Sigma^{21})^2}{Y_{\Sigma_1 \phi_3}} + \frac{(y_\Sigma^{22})^2}{Y_{\Sigma_2 \phi_3}} & \frac{y_\Sigma^{21} y_\Sigma^{31}}{Y_{\Sigma_1 \phi_3}} + \frac{y_\Sigma^{22} y_\Sigma^{32}}{Y_{\Sigma_2 \phi_3}} \\ \frac{y_\Sigma^{11} y_\Sigma^{31}}{Y_{\Sigma_1 \phi_3}} + \frac{y_\Sigma^{12} y_\Sigma^{32}}{Y_{\Sigma_2 \phi_3}} & \frac{y_\Sigma^{21} y_\Sigma^{31}}{Y_{\Sigma_1 \phi_3}} + \frac{y_\Sigma^{22} y_\Sigma^{32}}{Y_{\Sigma_2 \phi_3}} & \frac{(y_\Sigma^{31})^2}{Y_{\Sigma_1 \phi_3}} + \frac{(y_\Sigma^{32})^2}{Y_{\Sigma_2 \phi_3}} \end{pmatrix}. \quad (34)$$

This simplified light neutrino mass matrix also leads to a vanishing lightest neutrino mass while the three mixing angles can be satisfied by suitable tuning of the Yukawa couplings. Since for TeV scale triplet fermions, the Dirac Yukawa couplings $y_\Sigma^{\alpha\beta}$ have to be fine tuned at the level of $\leq 10^{-4}$, they do not impact the dark matter analysis discussed in this work. Hence, we do not take such couplings into our subsequent discussions.

IV. CONSTRAINTS ON THE MODEL PARAMETERS

Before going into the detailed calculation of DM relic abundance and relevant parameter scan, we note the existing theoretical as well as experimental constraints on the model parameters.

In order to keep the scalar potential (given in Eq. (14) within the square brackets) bounded from below, the quartic couplings must satisfy the following inequalities:

$$\begin{aligned} \lambda_H, \lambda_{\phi_1}, \lambda_{\phi_2}, \lambda_{\phi_3} &\geq 0, \\ \lambda_{H\phi_1} + \sqrt{\lambda_H \lambda_{\phi_1}} &\geq 0, \lambda_{H\phi_2} + \sqrt{\lambda_H \lambda_{\phi_2}} \geq 0, \\ \lambda_{H\phi_3} + \sqrt{\lambda_H \lambda_{\phi_3}} &\geq 0, \lambda_{\phi_1 \phi_2} + \sqrt{\lambda_{\phi_1} \lambda_{\phi_2}} \geq 0, \\ \lambda_{\phi_1 \phi_3} + \sqrt{\lambda_{\phi_1} \lambda_{\phi_3}} &\geq 0, \lambda_{\phi_2 \phi_3} + \sqrt{\lambda_{\phi_2} \lambda_{\phi_3}} \geq 0. \end{aligned} \quad (35)$$

To prevent perturbative breakdown of the model, all quartic, Yukawa and gauge couplings should obey the following limits at any energy scale:

$$\begin{aligned}
|\lambda_H| &< 4\pi, \quad |\lambda_{\phi_{1,2,3}}| < 4\pi, \quad |\lambda_{H\phi_{1,2,3}}| < 4\pi, \\
|\lambda_{\phi_1\phi_2}| &< 4\pi, \quad |\lambda_{\phi_1\phi_3}| < 4\pi, \quad |\lambda_{\phi_2\phi_3}| < 4\pi, \\
|\mathcal{Y}_i| &< \sqrt{4\pi}, \quad |Y_{\Sigma_{1,2}\phi_3}| < \sqrt{4\pi}, \quad |Y_{\Sigma_3\phi_2}| < \sqrt{4\pi}, \\
|Y_{\Sigma_{13}\phi_1}| &< \sqrt{4\pi}, \quad |Y_{\Sigma_{23}\phi_1}| < \sqrt{4\pi}, \quad |Y_{\Sigma_{12}\phi_3}| < \sqrt{4\pi} \\
|g, g'| &< \sqrt{4\pi}, \quad |g_{BL}| < \sqrt{4\pi},
\end{aligned} \tag{36}$$

Experimental limits from LEP II constrains such new gauge sector by putting a lower bound on the ratio of new gauge boson mass to the new gauge coupling $M_{Z'}/g' \geq 7$ TeV [104, 105]. The corresponding bounds from the LHC experiment have become stronger than this by now. Search for high mass dilepton resonances have put strong bounds on mass of such gauge boson coupling to first two generations of leptons with couplings similar to electroweak ones. The latest bounds from the ATLAS experiment [106, 107] and the CMS experiment [108] at the LHC rule out such gauge boson masses below 4-5 TeV from analysis of 13 TeV data. Such bounds get weaker, if the corresponding gauge couplings are weaker [106] than the electroweak gauge couplings. Also, if the Z' gauge boson couples only to the third generation of leptons, all such collider bounds become much weaker, as explored in the context of DM and collider searches in a recent work [109].

Similarly, the additional scalars in the model also face stringent constraints which typically arise due to their mixing with the SM Higgs boson which enable them to couple with the SM particles. The bound on such scalar mixing angles would come from both theoretical and experimental constraints [110, 111]. In case of scalar singlet extension of SM, the strongest bound on scalar-SM Higgs mixing angle ($\theta_{1j}, j = 2, 3, 4$) comes from W boson mass correction [112] at NLO for $250 \text{ GeV} \lesssim M_{s_i} \lesssim 850 \text{ GeV}$ as $(0.2 \lesssim \sin \theta_{1j} \lesssim 0.3)$ where M_{s_i} is the mass of other physical Higgs. Whereas, for $M_{s_i} > 850 \text{ GeV}$, the bounds from the requirement of perturbativity and unitarity of the theory turn dominant which gives $\sin \theta_{1j} \lesssim 0.2$. For lower values *i.e.* $M_{s_i} < 250 \text{ GeV}$, the LHC and LEP direct search [113, 114] and measured Higgs signal strength [114] restrict the mixing angle $\sin \theta_{1j}$ dominantly ($\lesssim 0.25$). The bounds from the measured value of EW precision parameter are mild for $M_{s_i} < 1 \text{ TeV}$. While these constraints restrict the singlet scalar mixing with SM Higgs denoted by $(\theta_{1j}, j = 2, 3, 4)$, the other three angles $(\theta_{23}, \theta_{24}, \theta_{34})$ remain unconstrained. We

choose our benchmark values of singlet scalar masses and their mixing with SM Higgs boson in such a way that these constraints are automatically satisfied.

V. THE BOLTZMANN EQUATIONS FOR TWO COMPONENT DM

In this work, as we already know that we are dealing with two stable dark matter candidates ξ_1 and ξ_2 . To find the present number densities of dark matter candidates we need to solve two Boltzmann equations one for each candidate. The collision term of each Boltzmann equation contains all possible number changing interactions of that particular dark matter candidate allowed by the symmetries. In the present model, there are two types of number changing interactions for a dark matter candidate. First one is the pair annihilation where ξ_i and $\bar{\xi}_i$ annihilate in a pair into all possible final states (X) except a pair of other dark matter candidate $\xi_j \bar{\xi}_j$ ($j \neq i$). These processes reduce the number of ξ_i and $\bar{\xi}_i$ by one unit (assuming there is no asymmetry in the number densities of dark matter and its anti-particle). The other type of number changing process is $\xi_i \bar{\xi}_i \rightarrow \xi_j \bar{\xi}_j$ ($i \neq j$). This is actually the conversion process where one type of dark matter converts into another. It increases the number of lighter dark matter candidate by two unit while reducing the number of heavier one by the same amount. This conversion process acts as a coupling between the individual Boltzmann equations of ξ_1 and ξ_2 . Let $n_2 = n_{\xi_2} + n_{\bar{\xi}_2}$ and $n_1 = n_{\xi_1} + n_{\bar{\xi}_1}$ are the total number densities of two dark matter candidates respectively. Assuming there is no asymmetry in number densities of ξ_i and $\bar{\xi}_i$, the two coupled Boltzmann equations in terms of n_2 and n_1 are given below [23, 115, 116],

$$\frac{dn_2}{dt} + 3n_2\mathbf{H} = -\frac{1}{2}\langle\sigma v_{\xi_2\bar{\xi}_2\rightarrow X\bar{X}}\rangle(n_2^2 - (n_2^{\text{eq}})^2) - \frac{1}{2}\langle\sigma v_{\xi_2\bar{\xi}_2\rightarrow\xi_1\bar{\xi}_1}\rangle\left(n_2^2 - \frac{(n_2^{\text{eq}})^2}{(n_1^{\text{eq}})^2}n_1^2\right), \quad (37)$$

$$\frac{dn_1}{dt} + 3n_1\mathbf{H} = -\frac{1}{2}\langle\sigma v_{\xi_1\bar{\xi}_1\rightarrow X\bar{X}}\rangle(n_1^2 - (n_1^{\text{eq}})^2) + \frac{1}{2}\langle\sigma v_{\xi_2\bar{\xi}_2\rightarrow\xi_1\bar{\xi}_1}\rangle\left(n_2^2 - \frac{(n_2^{\text{eq}})^2}{(n_1^{\text{eq}})^2}n_1^2\right), \quad (38)$$

where, n_i^{eq} is the equilibrium number density of dark matter species i . The second term in the left hand side involving the Hubble parameter \mathbf{H} represents dilution of number density due to the expansion of the Universe. The extra half factors in the collision term are due to non-self-conjugate (Dirac fermion) nature of our both dark matter candidates ξ_1 and ξ_2 [117]. Here we are more interested to study the evolution of number densities of two component WIMP system due to all possible interactions which change particle numbers of either ξ_1 or ξ_2 or both. Hence, in stead of actual number density n_i , it is convenient to describe the

Boltzmann equation for a species in terms of comoving number density $Y_i = n_i/s$ with s representing the entropy density of the Universe. The quantity Y_i is an useful one as it absorbs the effect of the expansion on n_i . In terms of comoving number densities, the above two coupled Boltzmann equations can be written as,

$$\frac{dY_2}{dx_{\xi_2}} = -\frac{1}{2}\sqrt{\frac{\pi}{45G}}\frac{m_{\xi_2}}{x_{\xi_2}^2}\sqrt{g_\star}\left(\langle\sigma v_{\xi_2\bar{\xi}_2\rightarrow X\bar{X}}\rangle(Y_2^2 - (Y_2^{\text{eq}})^2) + \langle\sigma v_{\xi_2\bar{\xi}_2\rightarrow\xi_1\bar{\xi}_1}\rangle\left(Y_2^2 - \frac{(Y_2^{\text{eq}})^2}{(Y_1^{\text{eq}})^2}Y_1^2\right)\right), \quad (39)$$

$$\frac{dY_1}{dx_{\xi_1}} = -\frac{1}{2}\sqrt{\frac{\pi}{45G}}\frac{m_{\xi_1}}{x_{\xi_1}^2}\sqrt{g_\star}\left(\langle\sigma v_{\xi_1\bar{\xi}_1\rightarrow X\bar{X}}\rangle(Y_1^2 - (Y_1^{\text{eq}})^2) - \langle\sigma v_{\xi_2\bar{\xi}_2\rightarrow\xi_1\bar{\xi}_1}\rangle\left(Y_2^2 - \frac{(Y_2^{\text{eq}})^2}{(Y_1^{\text{eq}})^2}Y_1^2\right)\right), \quad (40)$$

where, G is the Gravitational constant and $x_{\xi_i} = \frac{m_{\xi_i}}{T}$, is a dimensionless variable with T being the temperature of the Universe. The quantity g_\star is expressed as,

$$\sqrt{g_\star} = \frac{h_{\text{eff}}(T)}{\sqrt{g_{\text{eff}}(T)}}\left(1 + \frac{1}{3}\frac{d\ln(h_{\text{eff}}(T))}{d\ln(T)}\right), \quad (41)$$

where, $h_{\text{eff}}(T)$ and $g_{\text{eff}}(T)$ are the effective degrees of freedom related to the entropy and energy densities of radiation. In the collision term of the Boltzmann equation, the first term represents pair annihilations of ξ_i and $\bar{\xi}_i$ into particles which are in thermal equilibrium (including the SM particles also) while the second term is due to the dark matter conversion process $\xi_2\bar{\xi}_2 \rightarrow \xi_1\bar{\xi}_1$ where none of them are in thermal equilibrium during freeze-out. Detailed derivation of this term when both initial as well as final state particles are not in thermal contact with the visible world is given in Appendix C. In the collision term, the thermal averaged annihilation cross section of a particular process $AA' \rightarrow BB'$ has been denoted by $\langle\sigma v_{AA'\rightarrow BB'}\rangle$. The possible annihilation channels of both the DM candidates in our model are shown in figure 2. This figure not only contains the Feynman diagrams for individual DM annihilations into other particles, but also the conversion of one particular DM pair into a pair of the other DM. We have solved these two coupled Boltzmann equations using `micrOMEGAs` [118] where the model information has been supplied to `micrOMEGAs` using `FeynRules` [119]. All the relevant annihilation cross sections of dark matter number changing processes required to solve the coupled equations are calculated using `CalcHEP` [120]. Finally, after solving the Boltzmann equations we get the comoving number density $Y_i(T_0)$ of each dark matter candidate at the present epoch (at $T = T_0$). Thereafter, one can easily calculate the total dark matter relic density which is sum of relic densities of all dark

matter candidates,

$$\Omega_{\text{DM}} h^2 = 2.755 \times 10^8 \sum_{i=1}^2 \left(\frac{m_{\xi_i}}{\text{GeV}} \right) Y_i(T_0). \quad (42)$$

In order to understand how the comoving number densities are varying with respect to

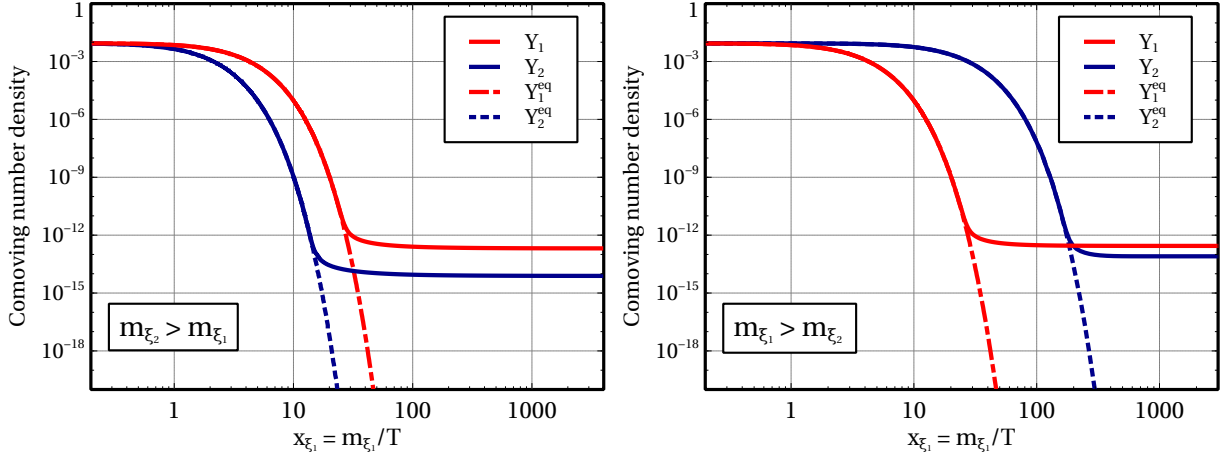


FIG. 1: Evolution of comoving number densities of both ξ_1 and ξ_2 for two cases (a) $m_{\xi_2} > m_{\xi_1}$ (left panel) and (b) $m_{\xi_1} > m_{\xi_2}$ (right panel).

the temperature T , we have shown two plots in the both panels of Fig. 1 illustrating the thermal evolution of Y_1 and Y_2 for $m_{\xi_2} > m_{\xi_1}$ (left panel) and $m_{\xi_1} > m_{\xi_2}$ (right panel) respectively. In the left panel, we consider $m_{\xi_2} = 2m_{\xi_1}$ with $m_{\xi_1} = 2110$ GeV. Here, the red solid line represents the variation of Y_1 with $x_{\xi_1} = \frac{m_{\xi_1}}{T}$ while the same for heavier component ξ_2 has been indicated by the blue solid line. The corresponding equilibrium number densities computed using the Maxwell-Boltzmann distribution are shown by red dash-dotted and blue dotted lines respectively. From this plot it is seen that initially for low x_{ξ_1} (i.e. for high T) the comoving number density of each component follows their respective equilibrium number density upto a certain temperature T (different for ξ_1 and ξ_2) and thereafter Y_i departs significantly from the corresponding equilibrium distribution function Y_i^{eq} and remains constant with respect to the variation of T . This is nothing but the well known freeze-out point of a WIMP and it depends on when the interaction rate corresponding to the number changing processes of a particular dark matter component goes below the expansion rate of the Universe governed by the Hubble parameter \mathbf{H} . In this particular situation, freeze-out of ξ_1 occurs at $x_{\xi_1} \sim 25$ while that for the heavier component is $\frac{m_{\xi_2}}{T} \sim 30$ ($x_{\xi_2} = 2x_{\xi_1}$). Furthermore, the interactions of ξ_1 and ξ_2 are such that ξ_2 which

freezes-out earlier has less relic abundance compared to its lighter counter part ξ_1 . The opposite situation is presented in the right panel of Fig. 1, where ξ_1 is the heavier dark matter component. Here we consider the model parameters in such a way that although the heavier component ξ_1 has earlier freeze-out, ends up with a greater abundance.

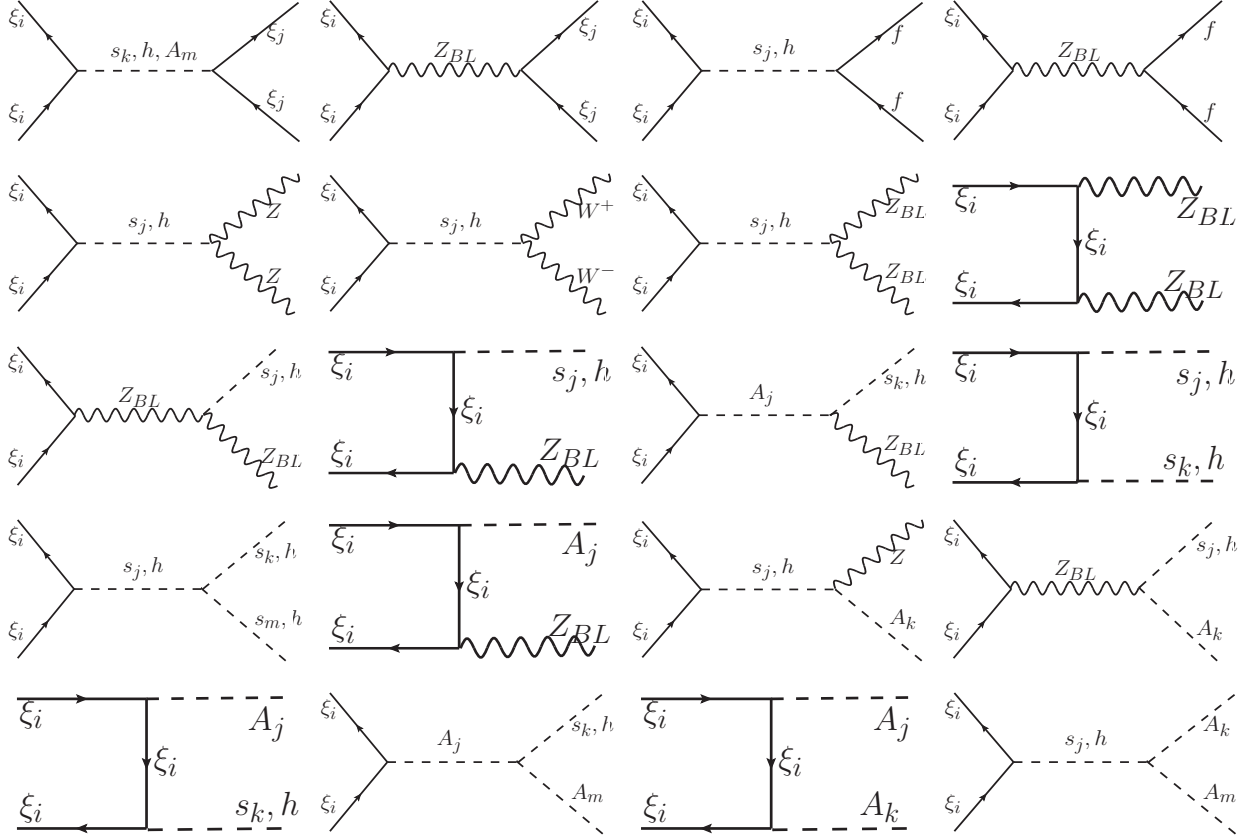


FIG. 2: Feynman diagrams for all possible annihilation channels of two DM candidates.

VI. DIRECT DETECTION

Since each of the DM candidates in our model is a Dirac fermion, there exists Z_{BL} as well as scalar mediated spin independent elastic scattering processes off nucleons. The relevant Feynman diagrams are shown in figure 3. Since several ongoing experiments like LUX [8], PandaX-II [9, 10] and Xenon1T [11, 12] are looking for such processes, regularly giving stringent upper bounds on DM-nucleon scattering cross section, we can further constrain our model parameters from these data. Parametrising DM and quark interactions with Z_{BL}

as

$$\mathcal{L} \supset [\bar{\xi}_i \gamma^\mu (g_{\xi_i v} + g_{\xi_1 a} \gamma^5) \xi_i + \bar{q} \gamma^\mu (g_{qv} + g_{qa} \gamma^5) q] (Z_{BL})_\mu,$$

the dominant spin independent DM-nucleus scattering cross section can be written down as [121]

$$\sigma_{\xi_i}^{\text{SI}} = \frac{\mu_{\xi_i N}^2 g_{\xi_i v}^2}{\pi M_{Z_{BL}}^4} [Z(2\tilde{b}_u + \tilde{b}_d) + (A - Z)(\tilde{b}_u + 2\tilde{b}_d)]^2 \quad (43)$$

where $\mu_{\xi_i N}$ is the reduced mass of DM nucleus system, \tilde{b}_q are the quark- Z_{BL} couplings which is same for all quarks in $B-L$ gauge model. Also, A, Z are mass number and atomic number of the nucleus. From the Lagrangian of DM given in (26), we can write

$$g_{\xi_1 v} = \frac{9}{10} g_{BL}, \quad g_{\xi_2 v} = \frac{4}{5} g_{BL}$$

which can be used in the expression above to find the DM-nucleus scattering cross section numerically for different values of $g_{BL}, M_{Z_{BL}}$. Similarly, if the scalar (s_j) mediated interactions are parametrised as

$$\mathcal{L} \supset [\bar{\xi}_i (\lambda_{\xi_i s} + \lambda_{\xi_1 p} \gamma^5) \xi_i + \bar{q} (\lambda_{qs} + \lambda_{qp} \gamma^5) q] s_j$$

the corresponding spin-independent DM-nucleus scattering cross section can be written as

$$\sigma_{\xi_i}^{\text{SI}} = \frac{\mu_{\xi_i N}^2 \lambda_{\xi_i s}^2}{\pi M_{s_j}^4} [Z \tilde{f}_p + (A - Z) \tilde{f}_n]^2. \quad (44)$$

Here $\tilde{f}_{p,n}$ are defined as

$$\frac{\tilde{f}_{p,n}}{m_{p,n}} = \sum_{q=u,d,s} f_{T_q}^{p,n} \frac{\tilde{f}_q}{m_q} + \frac{2}{27} f_{TG} \sum_{q=c,b,t} \frac{\tilde{f}_q}{m_q} \quad (45)$$

with $\tilde{f}_q = \lambda_{s_i} m_q / \text{GeV}$ and $f_{TG} = 1 - f_{T_u}^{p,n} - f_{T_d}^{p,n} - f_{T_d}^{n,n}$. Here λ_{s_i} denotes the quark-singlet scalar couplings which can be derived by using the singlet scalar-SM Higgs mixing shown in Appendix A. We take the standard values of other parameters appearing in the above formula as $f_{T_u}^p = 0.020$, $f_{T_d}^p = 0.026$ (and opposite for $f_{T_{u,d}}^n$), $f_{T_s} = 0.043$ which further gives $f_{TG} \approx 0.91$. We extract the spin independent elastic scattering cross section for both the DM candidates off nucleons from micrOMEGAs. Keeping the fact in mind that we are analysing a two-component DM scenario we have multiplied the elastic scattering cross-section by the relative number density of each DM candidate to find the individual effective DM-nucleon scattering cross section.

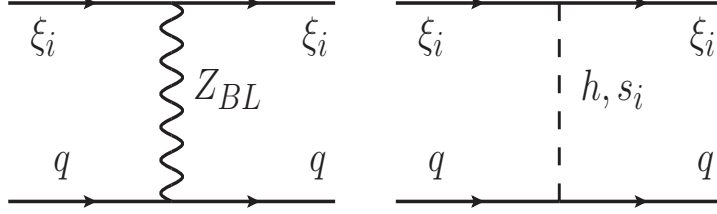


FIG. 3: Feynman diagrams for spin-independent elastic scattering processes of DM with nucleons (or quarks) in the model.

VII. RESULTS

As we have discussed in the previous section, this model predicts two automatically stable DM candidates ξ_1 and ξ_2 . The total relic density of DM can be expressed as, the sum of the relic densities of ξ_1 and ξ_2 , $\Omega_{\text{DM}} h^2 = \Omega_{\xi_1} h^2 + \Omega_{\xi_2} h^2$ where $\Omega_{\xi_1} h^2$ and $\Omega_{\xi_2} h^2$ are the relic abundances of ξ_1 and ξ_2 respectively. Let us now investigate the dependence of the relic densities, Ω_{ξ_1} and Ω_{ξ_2} , on the parameters of the model. In Figure 4, we have shown the variation of relic density with the DM mass by assuming $M_{\xi_2} = M_{\xi_1}$. The other parameters of the model were chosen as $M_{\psi_1} = 1.5$ TeV, $M_{\psi_2} = 2$ TeV, $M_{\psi_3} = 750$ GeV, $M_{s_1} = M_{s_2} = M_{s_3} = 1$ TeV, $M_{A_3} = 10$ TeV, $s_{12} = s_{13} = s_{14} = s_{24} = 0.2$, $M_{Z_{BL}} = 5$ TeV, $g_{BL} = 0.3$. The dashed (blue) and dotted (red) lines denote the relic densities of each DM candidate, $\Omega_{\xi_1} h^2$ and $\Omega_{\xi_2} h^2$, whereas the solid (green) line is their sum ($\Omega_{DM} h^2$). The horizontal magenta line represents the relic density bound from PLANCK data [3]. Some important features of the model can be indicated here. The resonances due to the s-channel annihilation through Z_{BL} and the different scalars (s_1, s_2, s_3, A_2, A_3) has reduced the relic density as expected. Figure 4 clearly shows four different scalars and Z_{BL} resonances, as we have assumed all the scalars have the same mass, at a DM mass of 500 GeV, 2.5 TeV, 3.27 TeV, and 5 TeV respectively. At DM mass of 1 TeV, DM particles starts annihilating into the two scalars final state giving a sudden reduction in the relic density. Similar behaviour can be found at the DM mass around 3.77 TeV, and 5.5 TeV where DM starts annihilating into one scalar ($M_{s_i} = 1$ TeV) plus one pseudo scalar ($M_{A_2} = \sqrt{\frac{3}{7}} M_{A_3} = 6.54$ TeV and $M_{A_3} = 10$ TeV) final states (Feynman diagrams in Figure 2). One can expect similar reduction for the annihilation into one scalar ($M_{s_i} = 1$ TeV) and one Z_{BL} ($M_{Z_{BL}} = 5$ TeV) final state near 3 TeV mass. However, because of the resonance that effect is not visible. Another important point to note here is that, Ω_{ξ_2}

is subdominant throughout the whole mass range. That can be explained as follows, ξ_2 has formed by combining N_{2L} and N_{2R} where as ξ_1 has formed from N_{1L} and N_{1R} . The $B - L$ quantum number assigned for N_{2L} and N_{2R} is greater than the quantum number for N_{1L} and N_{1R} and that increases the annihilation cross section of ξ_2 by some numerical factor which results to smaller abundance.

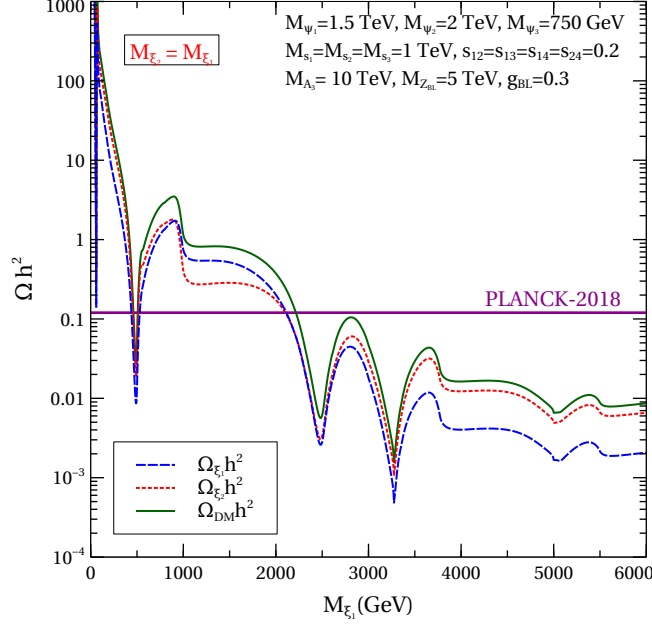


FIG. 4: Relic abundance of two DM candidates with degenerate masses keeping all other model parameters fixed to benchmark values.

In figure 5, we have shown the variation of the relic density for two different relations between M_{ξ_1} and M_{ξ_2} . In left panel, we have assumed $M_{\xi_2} = 2 M_{\xi_1}$ and in right panel $M_{\xi_2} = M_{\xi_1}/2$ – other parameters remain same as in figure 4. In figure 5a, the resonances have occurred at different positions for Ω_{ξ_2} , at 250 GeV, 1.25 TeV, 1.63 TeV, and 2.5 TeV, whereas, Ω_{ξ_1} has the same behaviour as in 4 which is expected as we have assumed the $M_{\xi_2} = 2 M_{\xi_1}$. Figure 5b can be explained in a similar way.

In figure 6 we have shown the variation of the total relic density as a function of m_{ξ_1} for three benchmark values of g_{BL} (0.01, 0.09, 0.4) and mixing angle (0.001, 0.01, 0.1). The left panel shows that the total DM abundance increases as we choose smaller values of gauge coupling. It is because small g will decrease the annihilation cross section and eventually increase the DM abundance. The right panel shows that the relic abundance hardly depends

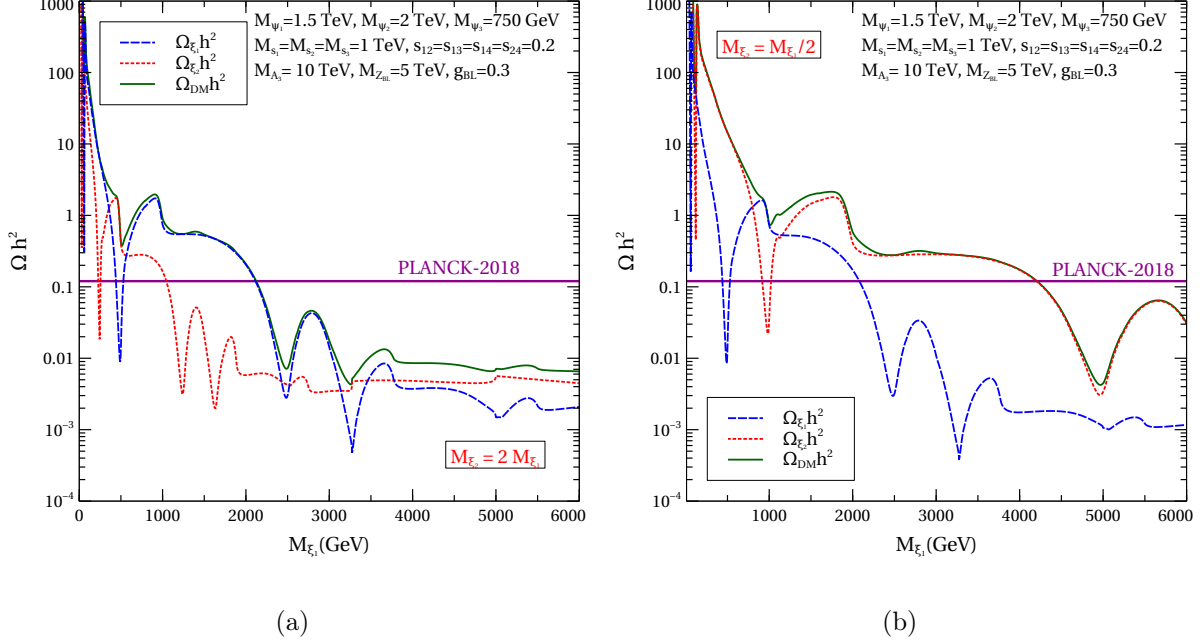


FIG. 5: Relic abundance of two DM candidates with non-degenerate masses: $M_{\xi_2} = 2M_{\xi_1}$ (left panel) and $M_{\xi_2} = M_{\xi_1}/2$ (right panel), keeping all other model parameters fixed to benchmark values.

on the mixing angle. Here for simplicity we have assumed all the mixing angle to be same. In both the cases, we have assumed $M_{\xi_2} = 2 M_{\xi_1}$ and the other parameters remain same as in figure 4.

As seen from the above plots, the relic abundance of both the DM candidates primarily depend upon the strength of their annihilation cross sections via scalar or gauge portal interactions. After understanding this behaviour from the plots with benchmark choices of model parameters, we now move onto performing a random scan over a set of free parameters mentioned in table III. While the physical masses of DM and all new particles in the model are varied in the mentioned range along with g_{BL} , the singlet scalar mixing angles with SM Higgs boson as well as among themselves are kept fixed at 0.2. We then apply the relevant constraints one by one to arrive at the final allowed parameter space from all relevant bounds. We first show the parameter space in $M_{\xi_1} - M_{\xi_2}$ plane allowed from total DM relic abundance, perturbativity, bounded from below criteria of the scalar potential in figure 7. In figure 8, we then show the parameter space in $g_{BL} - M_{Z_{BL}}$ plane allowed from total DM relic abundance, perturbativity, bounded from below criteria of the scalar potential. The bounds from the LEP and the LHC are separately shown by the respective shaded regions

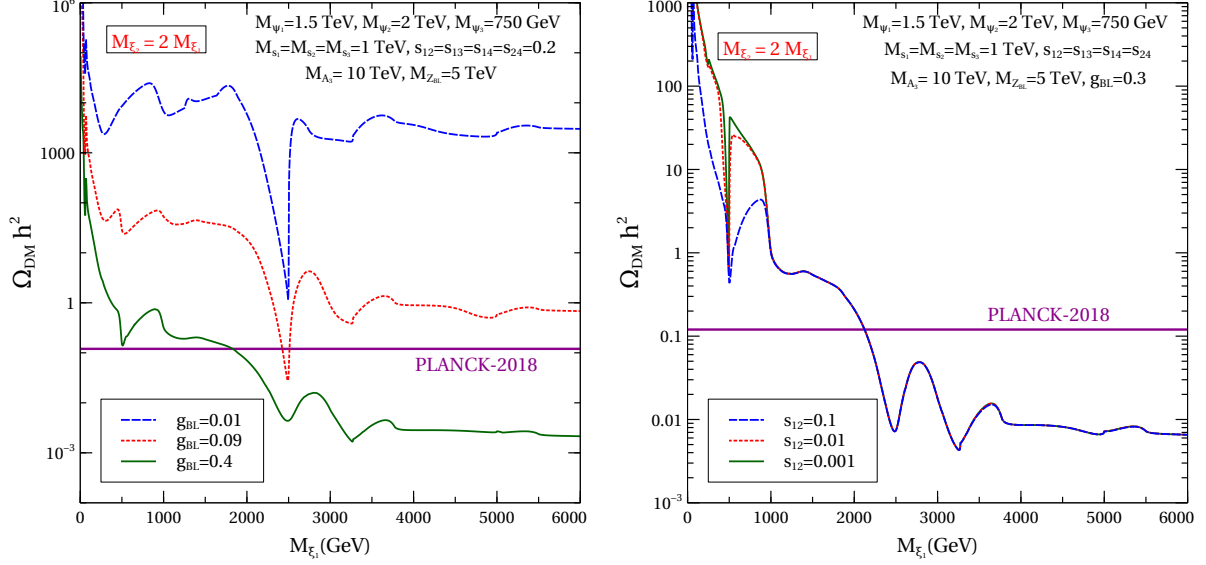


FIG. 6: Relic abundance of two DM candidates with non-degenerate masses ($M_{\xi_2} = 2M_{\xi_1}$) for different benchmark values of: gauge coupling g_{BL} (left panel), singlet scalar-SM Higgs mixing (right panel).

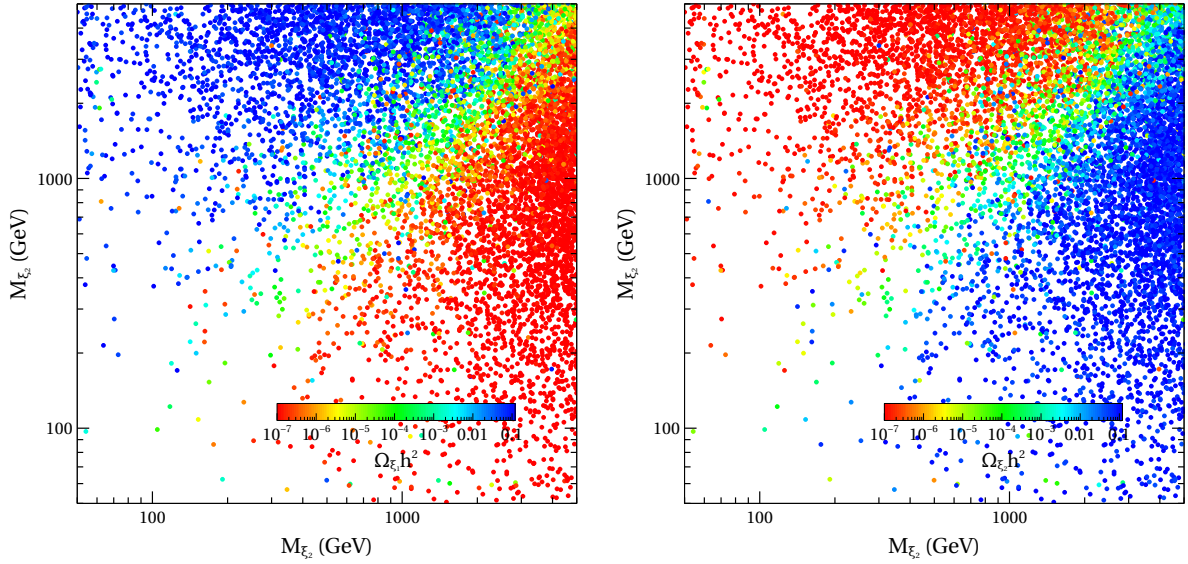


FIG. 7: Scan plot showing the parameter space in $M_{\xi_1} - M_{\xi_2}$ plane allowed from total DM relic abundance, perturbativity, bounded from below criteria of the scalar potential.

which are excluded. The coloured bar in the two plots shown in figure 8 correspond to the relative abundances of two DM candidates ξ_1 (left panel) and ξ_2 (right panel) respectively.

In figure 9, we show the spin independent DM-nucleon scattering cross section for in-

Parameters	Range
M_{ξ_1}	(10 GeV, 8 TeV)
M_{ξ_2}	(10 GeV, 8 TeV)
$M_{Z_{BL}}$	(100 GeV, 10 TeV)
g_{BL}	(0.0001, 1)
M_{s_1}	(100 GeV, 10 TeV)
M_{s_2}	(100 GeV, 10 TeV)
M_{s_3}	(100 GeV, 10 TeV)
M_{A_3}	(1 TeV, 20 TeV)
M_{A_2}	$\sqrt{\frac{3}{7}} M_{A_3}$
M_{ψ_3}	(1 TeV, 2.5 TeV)
M_{ψ_2}	$750 \text{ GeV} + M_{\psi_3}$
M_{ψ_1}	$1.5 \text{ TeV} + M_{\psi_3}$

TABLE III: The parameters of our model and ranges used in the random scan

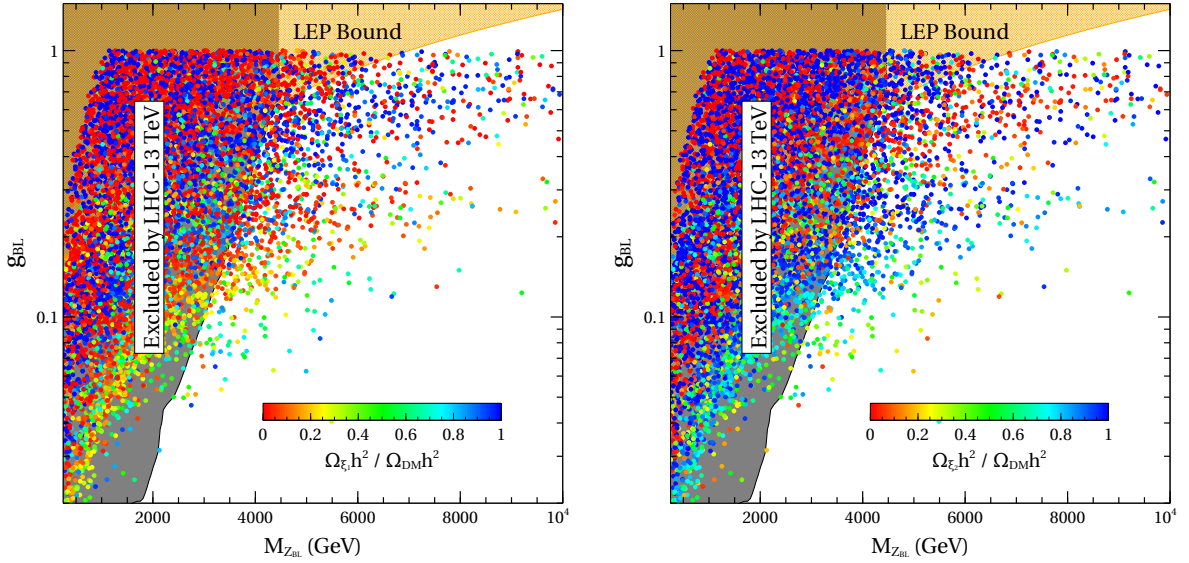


FIG. 8: Scan plot showing the parameter space in $g_{BL} - M_{Z_{BL}}$ plane allowed from total DM relic abundance, perturbativity, bounded from below criteria of the scalar potential.

dividual DM candidates as functions of their mass. All the points satisfy the total DM relic, perturbativity, bounded from below criteria of the scalar potential. As mentioned ear-

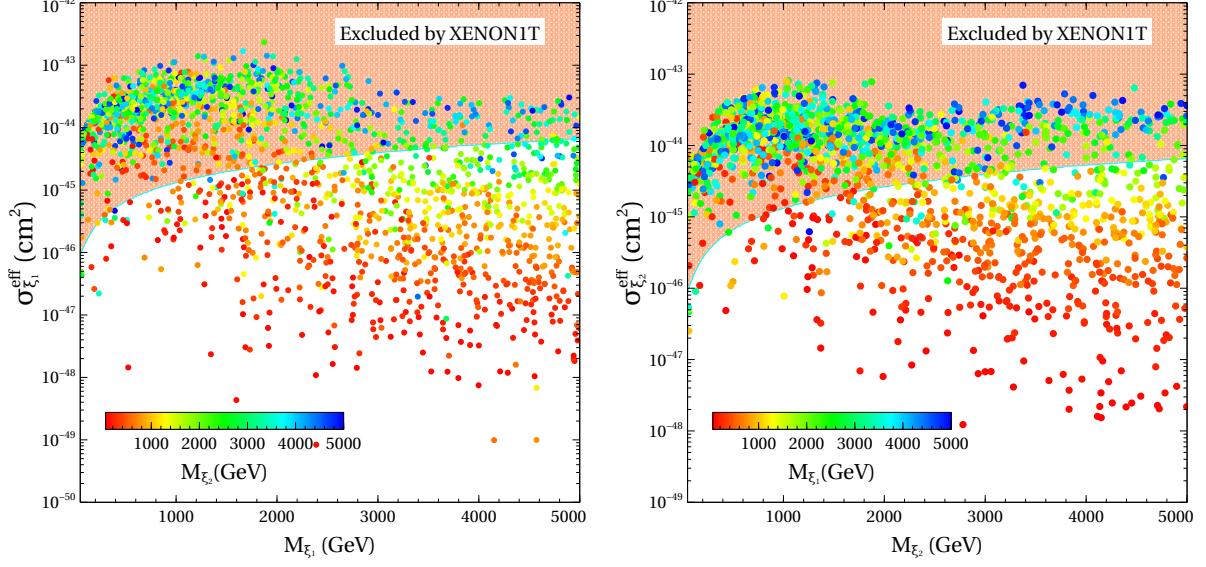


FIG. 9: Effective spin-independent scattering cross section off nucleons for individual DM candidates. All the points satisfy total DM relic, perturbativity, bounded from below criteria of the scalar potential.

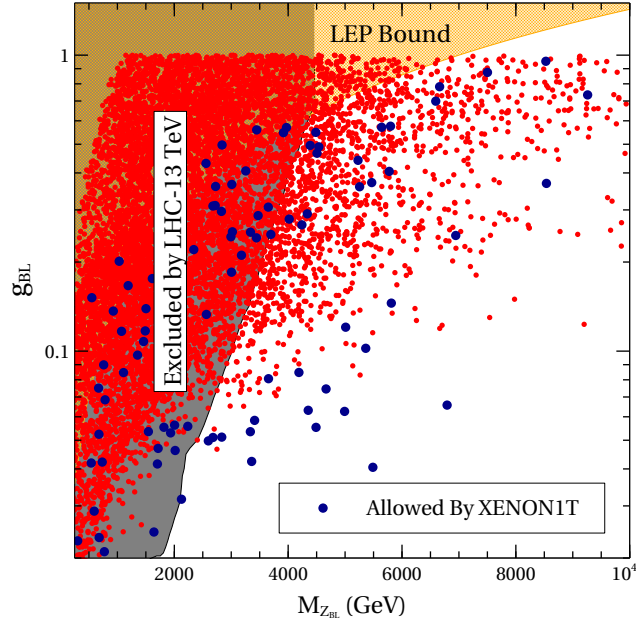


FIG. 10: Summary plot showing the allowed points with and without applying the direct detection bounds from XENON1T experiment.

lier, the actual scattering cross section is multiplied by individual relative number densities $n_{\xi_{1,2}}/(n_{\xi_1} + n_{\xi_2})$ in order to compare with the XENON1T bounds [12] derived for single DM

component. This clearly shows that the model remains very much sensitive to the direct detection experiments with many parts of parameter space already being ruled out. We then superimpose the collider bounds also on these points and show the resulting parameter space in figure 10. The severe impact of XENON1T constraints is clearly visible here with a very few points allowed compared to the points allowed without applying the XENON1T bounds. Although the individual DM-nucleon scattering bound allowed several points in the parameter space to survive, as seen from figure 9, when we impose the condition that both the DM candidates must satisfy the XENON1T bounds, it results in a much smaller allowed parameter space, seen in figure 10. The allowed points in the chosen range of random scan will face further constraints from future LHC runs as well as direct detection experiments like LZ [13], XENONnT [14], DARWIN [15] and PandaX-30T [16].

VIII. LHC SIGNATURES OF FERMION TRIPLETS

Although typical LHC signatures of a $U(1)_{B-L}$ model is via search for dilepton resonance mediated by Z_{BL} mentioned before, the present model can have additional prospects of being discovered at the LHC due to the presence of triplet fermions. While the neutral components of fermion triplets play the role of generating light neutrino masses through type III seesaw mechanism, the charged components can leave interesting signatures at colliders. We consider the third fermion triplet and its charged component as it can have enhanced production cross section at colliders due to larger $B-L$ charge. It should be noted that unlike in usual type III seesaw model, here the charged components of fermion triplets can be produced at the LHC via both Z and Z_{BL} gauge bosons, apart from usual photon mediation. The charged components can then decay into (i) charged lepton and Higgs boson or (ii) neutral fermion triplet plus on or off-shell W boson depending upon the mass splitting $\Delta M \gtrsim 80$ GeV or $\Delta M \lesssim 80$ GeV. Although the components of a particular fermion triplet have degenerate masses (M_{k0}) at tree level, one can make the charged components ψ_k^\pm heavier by considering one loop electroweak radiative corrections [122, 123], which result in a mass splitting $\Delta M \sim 166$ MeV between $M_{\psi_k^\pm}$ and $M_{\psi_k^0}$ for $M_{k0} \gtrsim 1$ TeV. Thus, in the second possible decay channel mentioned above, only the off-shell W boson is possible. The first decay mode is typically sub-dominant by the constraints from light neutrino masses, which require TeV scale fermion triplet Yukawa couplings with the SM leptons to be as small as

around $10^{-6} - 10^{-5}$. Therefore we consider the second decay mode only where the charged component of triplet decays into the neutral component and an off-shell W boson. Due to the small mass splitting, the dominant decay mode has final states ψ_k^0, π^\pm . The decay width of ψ_3^\pm to ψ_3^0 and π^\pm can be written as

$$\Gamma_{\psi_3^\pm \rightarrow \psi_3^0 \pi^\pm} = \frac{g^4 f_\pi^2 V_{ud}^2}{128\pi M_W^4 M_{\psi_3^\pm}} \Delta M^2 \left((M_{\psi_3^0} + M_{\psi_3^\pm})^2 - M_\pi^2 \right) \times \sqrt{1 - \frac{(M_{\psi_3^0} - M_\pi)^2}{M_{\psi_3^\pm}^2}} \sqrt{1 - \frac{(M_{\psi_3^0} + M_\pi)^2}{M_{\psi_3^\pm}^2}}, \quad (46)$$

where $\Delta M = M_{\psi_3^\pm} - M_{\psi_3^0} \simeq 166$ MeV, g is the $SU(2)_L$ gauge coupling, $f_\pi = 131$ MeV [122] is the pion decay constant, and the first diagonal element of the CKM matrix $V_{ud} \simeq 0.974$ respectively. Such tiny decay width keeps the lifetime of ψ_3^\pm considerably long enough so that it can reach the detector before decaying. In fact, the ATLAS experiment at the LHC has already searched for such long-lived charged particles with lifetime ranging from 10 ps to 10 ns, with maximum sensitivity around 1 ns [124]. In the decay $\psi_3^\pm \rightarrow \psi_3^0 \pi^\pm$, the final state pion typically has very low momentum and it is not reconstructed in the detector. On the other hand ψ_3^0 is a long lived particle as it can decay to SM leptons through the small mixing with the other triplet fermions and leaves the detector without interacting. Therefore, it gives rise to a signature where a charged particle leaves a track in the inner parts of the detector and then disappears leaving no tracks in the portions of the detector at higher radii.

Another crucial difference from usual type III seesaw extension of the SM is that here the production cross section of fermion triplets gets enhanced. The presence of Z_{BL} significantly increases the production cross-section of the charged ψ_3^\pm pairs at the collider. This is due to the fact that the decay of the BSM neutral gauge boson to the ψ_3^\pm now happens on-shell in contrast to models where this decay takes place off-shell via SM Z boson and photon. Also, as there is no negative interference between the Z and Z_{BL} mediated charged ψ_3^\pm production channels, hence the addition of new channel always improves the production cross-section. In order to illustrate this improvement, we first show the variation of production cross-section $\sigma_{pp \rightarrow \psi_3^+ \psi_3^-}$ in the left panel of figure 11 for two different choices of centre of mass energy. As can be seen, the improvement in production cross section is more significant in 100 TeV centre of mass energies of proton proton collisions. Once produced, ψ_3^\pm can give rise to disappearing charged track signatures mentioned above. The ATLAS experiment at the

LHC put constraints on such disappearing charged track signatures for a long lived chargino decaying into a pion and wino dark matter, which is shown as the solid black line in right panel of figure 11. Although ψ_3^0 is not the DM candidate in our model, it effectively behaves like one at the LHC due to its long life. It can be seen that the existing LHC constraint can already rule out ψ_3^\pm masses below 500 GeV from its searches for disappearing charged tracks, keeping the parameter space considered in this study within near future sensitivity. Also, the bounds will get slightly tighter in our model due to enhanced production cross section. We leave a detailed study of such type III seesaw signatures at the LHC in the framework of a $B - L$ gauge model.

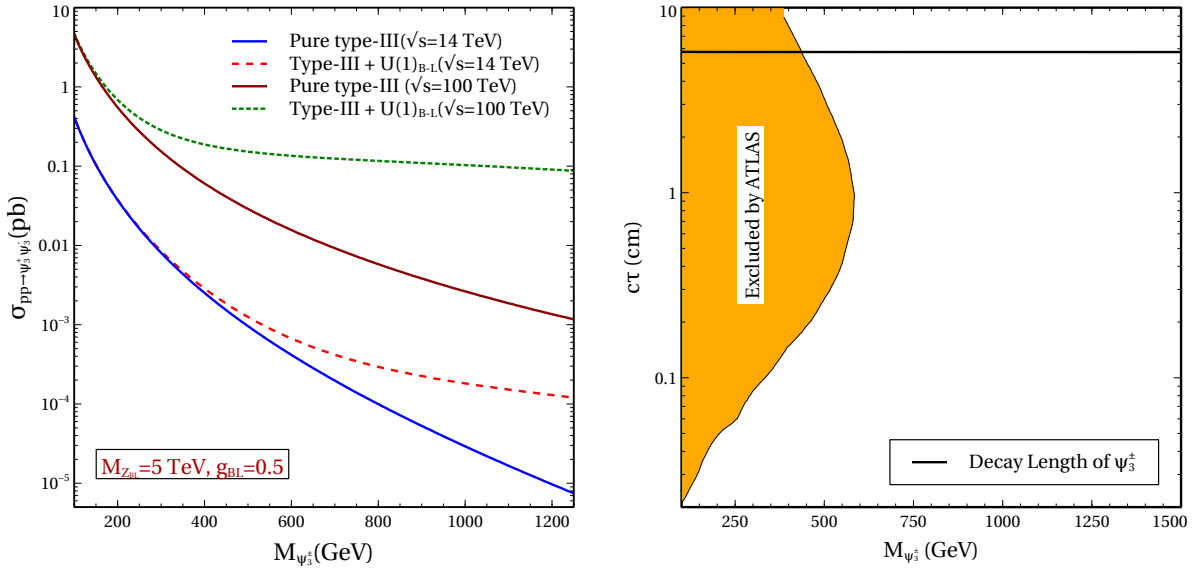


FIG. 11: Left panel: Plot showing improvement in production cross-section of the ψ_3^\pm pairs due to Z_{BL} mediation for two choices of centre of mass energies in proton proton collisions. Right panel: Decay length of ψ_3^\pm versus its mass compared with the ATLAS bound on disappearing charge track searches at 13 TeV centre of mass energy.

IX. CONCLUSION

We have proposed a gauged $U(1)_{B-L}$ version of type III seesaw model which naturally predicts a two component Dirac fermion dark matter scenario due to the requirements of anomaly cancellation. Unlike type I seesaw scenario in $U(1)_{B-L}$ model where three right handed singlet neutrinos with $B - L$ charge -1 each leads to cancelation of all anomalies

without any need of additional chiral fermions, type III seesaw implementation leads to additional anomalies due to the non-trivial $SU(2)_L$ structure of triplet fermions. We show that a gauged $U(1)_{B-L}$ model with three fermion triplets required for type III seesaw can be anomaly free due to the presence of two neutral Dirac fermions having fractional $B - L$ charges. Both of these fermions are naturally stable due to a remnant $\mathbb{Z}_2 \times \mathbb{Z}'_2$ symmetry. We study the DM phenomenology of the two component DM scenario in the model after incorporating all relevant theoretical and experimental bounds. Among the theoretical bounds, the bounded from below criteria of the scalar potential plays a crucial role restricting the parameter space. The relic abundance of the DM candidates are primarily dictated by their annihilations into SM particles mediated by Z_{BL} as well as additional singlet scalars. We find the parameter space allowed from total relic abundance criteria and then apply the bounds from direct detection experiments on individual DM candidates. We find that all these constraints tightly constrain the parameter space which we scan through in our study, leaving a small region which can be probed at experiments operational at different frontiers. Finally we comment upon one interesting prospect of probing this model through production of charged components of fermion triplets at colliders. The presence of additional neutral gauge boson Z_{BL} can significantly enhance the production cross section of charged triplets at LHC or 100 TeV future proton proton collider compared to usual type III seesaw extension of standard model. The charged components can then decay into the neutral ones and a pion with a long decay lifetime, leaving a disappearing charged track signature. Comparing with the ATLAS bounds on such signatures, we find that such triplets with masses upto 500 GeV or so can already be ruled out. While the charged components of fermion triplets can be probed via such disappearing charged track signatures, the neutral components, if long lived enough could be probed at proposed future experiments like MATHUSLA [125]. These triplets, however, do not affect the DM phenomenology much apart from opening another DM annihilation channel to triplet fermions whenever allowed kinematically.

Acknowledgments

DB acknowledges the support from IIT Guwahati start-up grant (reference number: xPHYSUGI-ITG01152xxDB001), Early Career Research Award from DST-SERB, Government of India (reference number: ECR/2017/001873) and Associateship Programme of Inter

University Centre for Astronomy and Astrophysics (IUCAA), Pune. DN would like to thank Rashidul Islam and Claude Duhr for various discussions regarding the implementation of the model in FeynRules. He would also like to thank Lopamudra Mukherjee and Suruj Jyoti Das for using their computers while doing the numerical scans.

Appendix A: Diagonalisation of mass matrix of real scalars

In this section we have listed all the elements of the diagonalising matrix \mathcal{O} of \mathcal{M}_{rs} in terms of mixing angles under the assumption that all the mixing angles among the singlet scalars are identical and equal to θ_{24} :

$$\begin{aligned}
\mathcal{O}_{11} &= c_{12} c_{13} c_{14}, \\
\mathcal{O}_{12} &= c_{13} c_{14} s_{12}, \\
\mathcal{O}_{13} &= c_{14} s_{13}, \\
\mathcal{O}_{14} &= s_{14}, \\
\mathcal{O}_{21} &= -c_{12} c_{13} s_{14} s_{24} - c_{12} c_{24} s_{13} s_{24} - c_{24}^2 s_{12}, \\
\mathcal{O}_{22} &= c_{12} c_{24}^2 - c_{13} s_{12} s_{14} s_{24} - c_{24} s_{12} s_{13} s_{24}, \\
\mathcal{O}_{23} &= c_{13} c_{24} s_{24} - s_{13} s_{14} s_{24}, \\
\mathcal{O}_{24} &= c_{14} s_{24}, \\
\mathcal{O}_{31} &= -c_{12} c_{13} c_{24} s_{14} s_{24} - c_{12} c_{24}^2 s_{13} + c_{12} s_{13} s_{24}^3 + c_{24} s_{12} s_{24}^2 + c_{24} s_{12} s_{24}, \\
\mathcal{O}_{32} &= -c_{24} (c_{12} s_{24}^2 + c_{24} s_{12} s_{13}) - c_{12} c_{24} s_{24} + s_{12} s_{24} (s_{13} s_{24}^2 - c_{13} c_{24} s_{14}), \\
\mathcal{O}_{33} &= c_{13} c_{24}^2 - c_{13} s_{24}^3 - c_{24} s_{13} s_{14} s_{24}, \\
\mathcal{O}_{34} &= c_{14} c_{24} s_{24}, \\
\mathcal{O}_{41} &= s_{12} (c_{24}^2 s_{24} - s_{24}^2) + c_{12} (-c_{13} c_{24}^2 s_{14} + s_{13} (c_{24} s_{24} + c_{24} s_{24}^2)), \\
\mathcal{O}_{42} &= -c_{13} c_{24}^2 s_{12} s_{14} + c_{12} (-c_{24}^2 s_{24} + s_{24}^2) + s_{12} s_{13} (c_{24} s_{24} + c_{24} s_{24}^2), \\
\mathcal{O}_{43} &= -c_{24}^2 s_{13} s_{14} - c_{13} (c_{24} s_{24} + c_{24} s_{24}^2), \\
\mathcal{O}_{44} &= c_{14} c_{24}^2.
\end{aligned}$$

Here, we have denoted $c_{ij} \equiv \cos \theta_{ij}$ and $s_{ij} \equiv \sin \theta_{ij}$ respectively. Now, using the elements of the diagonalising matrix, the physical scalar fields can be expressed as a linear combinations

of unphysical states as

$$h = \mathcal{O}_{11}h' + \mathcal{O}_{21}s'_1 + \mathcal{O}_{31}s'_2 + \mathcal{O}_{41}s'_3, \quad (\text{A1})$$

$$s_1 = \mathcal{O}_{12}h' + \mathcal{O}_{22}s'_1 + \mathcal{O}_{32}s'_2 + \mathcal{O}_{42}s'_3, \quad (\text{A2})$$

$$s_2 = \mathcal{O}_{13}h' + \mathcal{O}_{23}s'_1 + \mathcal{O}_{33}s'_2 + \mathcal{O}_{43}s'_3, \quad (\text{A3})$$

$$s_3 = \mathcal{O}_{14}h' + \mathcal{O}_{24}s'_1 + \mathcal{O}_{34}s'_2 + \mathcal{O}_{44}s'_3. \quad (\text{A4})$$

Appendix B: Diagonalisation of mass matrix of pseudo scalars

The pseudo scalar mass matrix with respect to the basis state $\frac{1}{\sqrt{2}}(A'_1 \ A'_2 \ A'_3)^T$ is given by

$$\mathcal{M}_{ps} = \begin{pmatrix} -2u(u\beta + \sqrt{2}\delta) & u^2\beta & u(-u\beta + \sqrt{2}\delta) \\ u^2\beta & -\frac{u}{2}(u\beta + \sqrt{2}\zeta) & \frac{u}{2}(u\beta + 2\sqrt{2}\zeta) \\ u(-u\beta + \sqrt{2}\delta) & \frac{u}{2}(u\beta + 2\sqrt{2}\zeta) & -\frac{u}{2}(u\beta + \sqrt{2}(\delta + 4\zeta)) \end{pmatrix}.$$

As expected, the pseudo scalar mass matrix is also real symmetric. Therefore, the matrix \mathcal{M}_{ps} can be diagonalised by a 3×3 orthogonal matrix and the corresponding eigenvalues are given below,

$$\begin{aligned} m_{A_1}^2 &= 0, \\ m_{A_2}^2 &= \frac{-6\beta u^4 - 5\sqrt{2}u^3(\delta + \zeta) + \sqrt{2}\sqrt{u^6(25\delta^2 - 34\delta\zeta + 25\zeta^2 + 18\beta^2u^2 - 12\sqrt{2}\beta u(\delta + \zeta))}}{4u^2}, \\ m_{A_3}^2 &= -\frac{6\beta u^4 + 5\sqrt{2}u^3(\delta + \zeta) + \sqrt{2}\sqrt{u^6(25\delta^2 - 34\delta\zeta + 25\zeta^2 + 18\beta^2u^2 - 12\sqrt{2}\beta u(\delta + \zeta))}}{4u^2}. \end{aligned} \quad (\text{B1})$$

Appendix C: Collision term of the Boltzmann equation for dark matter conversion process $\xi_2\bar{\xi}_2 \rightarrow \xi_1\bar{\xi}_1$

In this section, we have derived the Boltzmann equation for an interaction which converts one type of dark matter into another i.e. $\xi_2\bar{\xi}_2 \rightarrow \xi_1\bar{\xi}_1$. In this process, both initial and final states particles are dark matter candidates which are not in thermal equilibrium during and after their freeze-out. The situation is completely different when each type of dark matter annihilates into the SM particles in thermal equilibrium. The collision term of the

Boltzmann equations depends strongly on whether the final state particles in a scattering process are in thermal contact with thermal bath of the Universe or not. This actually modifies the form of the collision term which reduces to the known form when outgoing particles are in thermal equilibrium. The contribution of the process $\xi_2 \bar{\xi}_2 \rightarrow \xi_1 \bar{\xi}_1$ to the collision term of ξ_2 is given by

$$-\frac{g_{\xi_2}}{(2\pi)^3} \int \frac{\mathcal{C}[f_{\xi_2}]}{E_{\xi_2}} d^3 \vec{p}_{\xi_2}, \quad (\text{C1})$$

$$= - \int d\Pi_{\xi_2} d\Pi_{\bar{\xi}_2} d\Pi_{\xi_1} d\Pi_{\bar{\xi}_1} (2\pi)^4 \delta^4(p_{\xi_2} + p_{\bar{\xi}_2} - p_{\xi_1} - p_{\bar{\xi}_1}) |\mathcal{M}_{\xi_2 \bar{\xi}_2 \rightarrow \xi_1 \bar{\xi}_1}|^2 \times \\ \left(f_{\xi_2}(|\vec{p}_{\xi_2}|, T) f_{\bar{\xi}_2}(|\vec{p}_{\bar{\xi}_2}|, T) - f_{\xi_1}(|\vec{p}_{\xi_1}|, T) f_{\bar{\xi}_1}(|\vec{p}_{\bar{\xi}_1}|, T) \right), \quad (\text{C2})$$

where, p_i is the four momentum of species i while the corresponding three momentum and energy are denoted by \vec{p}_i and E_i respectively. The phase space factor $d\Pi_i \equiv \frac{g_i d^3 \vec{p}_i}{(2\pi)^3 E_i}$ with g_i is the internal degrees of freedom of species i having distribution function $f_i(|\vec{p}_i|, T)$. Here we have neglected the factors related to Pauli blocking for fermions (dark matter candidates) as those are not significant enough for the present context. Furthermore, $|\mathcal{M}_{\xi_2 \bar{\xi}_2 \rightarrow \xi_1 \bar{\xi}_1}|^2$ is the Feynman amplitude square of the concerned process $\xi_2 \bar{\xi}_2 \rightarrow \xi_1 \bar{\xi}_1$ and it is spin-averaged over both initial and final states particles. The above collision term can also be as

$$- \int d\Pi_{\xi_2} d\Pi_{\bar{\xi}_2} \int d\Pi_{\xi_1} d\Pi_{\bar{\xi}_1} (2\pi)^4 \delta^4(p_{\xi_2} + p_{\bar{\xi}_2} - p_{\xi_1} - p_{\bar{\xi}_1}) |\mathcal{M}_{\xi_2 \bar{\xi}_2 \rightarrow \xi_1 \bar{\xi}_1}|^2 \exp\left(-\frac{E_{\xi_2} + E_{\bar{\xi}_2}}{T}\right) \times \\ \left(\frac{f_{\xi_2}(|\vec{p}_{\xi_2}|, T)}{\exp\left(-\frac{E_{\xi_2}}{T}\right)} \frac{f_{\bar{\xi}_2}(|\vec{p}_{\bar{\xi}_2}|, T)}{\exp\left(-\frac{E_{\bar{\xi}_2}}{T}\right)} - \frac{f_{\xi_1}(|\vec{p}_{\xi_1}|, T)}{\exp\left(-\frac{E_{\xi_1}}{T}\right)} \frac{f_{\bar{\xi}_1}(|\vec{p}_{\bar{\xi}_1}|, T)}{\exp\left(-\frac{E_{\bar{\xi}_1}}{T}\right)} \right). \quad (\text{C3})$$

In the denominator of the last term, we have used the energy conservation condition i.e. $E_{\xi_2} + E_{\bar{\xi}_2} = E_{\xi_1} + E_{\bar{\xi}_1}$. The distribution function of a dark matter species ξ_i which not in equilibrium (both thermally as well as chemically) can be written as $f_{\xi_i} = \exp\left(\frac{\mu_{\xi_i} - E_{\xi_i}}{T}\right)$ with chemical potential $\mu_{\xi_i} \neq 0$ and $\mu_{\xi_i} = 0$ represents the equilibrium distribution function of ξ_i which is just $f_{\xi_i}^{\text{eq}} = \exp\left(-\frac{E_{\xi_i}}{T}\right)$. Therefore, one can easily show that $\frac{f_{\xi_i}}{f_{\xi_i}^{\text{eq}}} = \frac{n_{\xi_i}}{n_{\xi_i}^{\text{eq}}}$, where the number density $n_{\xi_i}^{\text{(eq)}}$ is defined as

$$n_{\xi_i}^{\text{(eq)}} = \frac{g_{\xi_i}}{(2\pi)^3} \int f_{\xi_i}^{\text{(eq)}} d^3 \vec{p}_{\xi_i}. \quad (\text{C4})$$

Using this, the terms within the brackets in Eq. (C3) can be replaced by number densities of ξ_1 and ξ_2 as

$$- \int d\Pi_{\xi_2} d\Pi_{\bar{\xi}_2} \left\{ \int d\Pi_{\xi_1} d\Pi_{\bar{\xi}_1} (2\pi)^4 \delta^4(p_{\xi_2} + p_{\bar{\xi}_2} - p_{\xi_1} - p_{\bar{\xi}_1}) |\mathcal{M}_{\xi_2 \bar{\xi}_2 \rightarrow \xi_1 \bar{\xi}_1}|^2 \right\} \times \exp\left(-\frac{E_{\xi_2} + E_{\bar{\xi}_2}}{T}\right) \left(\frac{n_{\xi_2}}{n_{\xi_2}^{\text{eq}}} \frac{n_{\bar{\xi}_2}}{n_{\bar{\xi}_2}^{\text{eq}}} - \frac{n_{\xi_1}}{n_{\xi_1}^{\text{eq}}} \frac{n_{\bar{\xi}_1}}{n_{\bar{\xi}_1}^{\text{eq}}} \right). \quad (\text{C5})$$

Now, the quantity within the curly brackets is equal to $4\sigma v E_{\xi_2} E_{\bar{\xi}_2}$ with σ being the annihilation cross section of $\xi_2 \bar{\xi}_2 \rightarrow \xi_1 \bar{\xi}_1$. Substituting this in the above we get

$$- \left\{ \frac{1}{n_{\xi_2}^{\text{eq}} n_{\bar{\xi}_2}^{\text{eq}}} \int \frac{d^3 \vec{p}_{\xi_2}}{(2\pi)^3} \frac{d^3 \vec{p}_{\bar{\xi}_2}}{(2\pi)^3} (\sigma v)_{\xi_2 \bar{\xi}_2 \rightarrow \xi_1 \bar{\xi}_1} \exp\left(-\frac{E_{\xi_2} + E_{\bar{\xi}_2}}{T}\right) \right\} \times \left(n_{\xi_2} n_{\bar{\xi}_2} - \frac{n_{\xi_2}^{\text{eq}}}{n_{\xi_1}^{\text{eq}}} \frac{n_{\bar{\xi}_2}^{\text{eq}}}{n_{\bar{\xi}_1}^{\text{eq}}} n_{\xi_1} n_{\bar{\xi}_1} \right), \quad (\text{C6})$$

where, the quantity within curly brackets is the thermal averaged cross section $\langle \sigma v_{\xi_2 \bar{\xi}_2 \rightarrow \xi_1 \bar{\xi}_1} \rangle$. Therefore, in terms of the thermal averaged cross section, the collision term of ξ_2 due to dark matter conversion process is given by

$$- \langle \sigma v_{\xi_2 \bar{\xi}_2 \rightarrow \xi_1 \bar{\xi}_1} \rangle \left(n_{\xi_2} n_{\bar{\xi}_2} - \frac{n_{\xi_2}^{\text{eq}}}{n_{\xi_1}^{\text{eq}}} \frac{n_{\bar{\xi}_2}^{\text{eq}}}{n_{\bar{\xi}_1}^{\text{eq}}} n_{\xi_1} n_{\bar{\xi}_1} \right). \quad (\text{C7})$$

In this work, we have assumed that there is no asymmetry between the number densities of dark matter candidate ξ_i and its antiparticle $\bar{\xi}_i$ and therefore, $n_{\xi_i}^{(\text{eq})} = n_{\bar{\xi}_i}^{(\text{eq})}$. Hence, the contribution of $\xi_2 \bar{\xi}_2 \rightarrow \xi_1 \bar{\xi}_1$ to the collision term of ξ_2 is given by

$$- \langle \sigma v_{\xi_2 \bar{\xi}_2 \rightarrow \xi_1 \bar{\xi}_1} \rangle \left\{ n_{\xi_2}^2 - \left(\frac{n_{\xi_2}^{\text{eq}}}{n_{\xi_1}^{\text{eq}}} \right)^2 n_{\xi_1}^2 \right\}, \quad (\text{C8})$$

while the collision term of ξ_1 also has an additional contribution which is exactly identical to the above except the overall $-ve$ sign will be replaced by a $+ve$ sign as the dark matter conversion process $\xi_2 \bar{\xi}_2 \rightarrow \xi_1 \bar{\xi}_1$ increases the number densities of both ξ_1 and $\bar{\xi}_1$.

-
- [1] **Particle Data Group** Collaboration, M. Tanabashi et al., *Review of Particle Physics*, *Phys. Rev.* **D98** (2018), no. 3 030001.
- [2] I. Esteban, M. C. Gonzalez-Garcia, A. Hernandez-Cabezudo, M. Maltoni, and T. Schwetz, *Global analysis of three-flavour neutrino oscillations: synergies and tensions in the determination of θ_{23} , δ_{CP} , and the mass ordering*, *JHEP* **01** (2019) 106, [[arXiv:1811.05487](#)].
- [3] **Planck** Collaboration, N. Aghanim et al., *Planck 2018 results. VI. Cosmological parameters*, [arXiv:1807.06209](#).
- [4] F. Zwicky, *Die Rotverschiebung von extragalaktischen Nebeln*, *Helv. Phys. Acta* **6** (1933) 110–127. [Gen. Rel. Grav.41,207(2009)].
- [5] V. C. Rubin and W. K. Ford, Jr., *Rotation of the Andromeda Nebula from a Spectroscopic Survey of Emission Regions*, *Astrophys. J.* **159** (1970) 379–403.
- [6] D. Clowe, M. Bradac, A. H. Gonzalez, M. Markevitch, S. W. Randall, C. Jones, and D. Zaritsky, *A direct empirical proof of the existence of dark matter*, *Astrophys. J.* **648** (2006) L109–L113, [[astro-ph/0608407](#)].
- [7] E. W. Kolb and M. S. Turner, *The Early Universe*, *Front. Phys.* **69** (1990) 1–547.
- [8] **LUX** Collaboration, D. S. Akerib et al., *Results from a search for dark matter in the complete LUX exposure*, *Phys. Rev. Lett.* **118** (2017), no. 2 021303, [[arXiv:1608.07648](#)].
- [9] **PandaX-II** Collaboration, A. Tan et al., *Dark Matter Results from First 98.7 Days of Data from the PandaX-II Experiment*, *Phys. Rev. Lett.* **117** (2016), no. 12 121303, [[arXiv:1607.07400](#)].
- [10] **PandaX-II** Collaboration, X. Cui et al., *Dark Matter Results From 54-Ton-Day Exposure of PandaX-II Experiment*, [arXiv:1708.06917](#).
- [11] **XENON** Collaboration, E. Aprile et al., *First Dark Matter Search Results from the XENON1T Experiment*, [arXiv:1705.06655](#).
- [12] E. Aprile et al., *Dark Matter Search Results from a One Tonne \times Year Exposure of XENON1T*, [arXiv:1805.12562](#).
- [13] **LZ** Collaboration, D. S. Akerib et al., *LUX-ZEPLIN (LZ) Conceptual Design Report*, [arXiv:1509.02910](#).

- [14] **XENON** Collaboration, E. Aprile et al., *Physics reach of the XENON1T dark matter experiment*, *JCAP* **1604** (2016), no. 04 027, [[arXiv:1512.07501](#)].
- [15] **DARWIN** Collaboration, J. Aalbers et al., *DARWIN: towards the ultimate dark matter detector*, *JCAP* **1611** (2016) 017, [[arXiv:1606.07001](#)].
- [16] J. Liu, X. Chen, and X. Ji, *Current status of direct dark matter detection experiments*, *Nature Phys.* **13** (2017), no. 3 212–216, [[arXiv:1709.00688](#)].
- [17] F. Kahlhoefer, *Review of LHC Dark Matter Searches*, *Int. J. Mod. Phys.* **A32** (2017), no. 13 1730006, [[arXiv:1702.02430](#)].
- [18] **Fermi-LAT, MAGIC** Collaboration, M. L. Ahnen et al., *Limits to dark matter annihilation cross-section from a combined analysis of MAGIC and Fermi-LAT observations of dwarf satellite galaxies*, *JCAP* **1602** (2016), no. 02 039, [[arXiv:1601.06590](#)].
- [19] Q.-H. Cao, E. Ma, J. Wudka, and C. P. Yuan, *Multipartite dark matter*, [arXiv:0711.3881](#).
- [20] K. M. Zurek, *Multi-Component Dark Matter*, *Phys. Rev.* **D79** (2009) 115002, [[arXiv:0811.4429](#)].
- [21] D. Chialva, P. S. B. Dev, and A. Mazumdar, *Multiple dark matter scenarios from ubiquitous stringy throats*, *Phys. Rev.* **D87** (2013), no. 6 063522, [[arXiv:1211.0250](#)].
- [22] J. Heeck and H. Zhang, *Exotic Charges, Multicomponent Dark Matter and Light Sterile Neutrinos*, *JHEP* **05** (2013) 164, [[arXiv:1211.0538](#)].
- [23] A. Biswas, D. Majumdar, A. Sil, and P. Bhattacharjee, *Two Component Dark Matter : A Possible Explanation of 130 GeV γ - Ray Line from the Galactic Centre*, *JCAP* **1312** (2013) 049, [[arXiv:1301.3668](#)].
- [24] S. Bhattacharya, A. Drozd, B. Grzadkowski, and J. Wudka, *Two-Component Dark Matter*, *JHEP* **10** (2013) 158, [[arXiv:1309.2986](#)].
- [25] L. Bian, R. Ding, and B. Zhu, *Two Component Higgs-Portal Dark Matter*, *Phys. Lett.* **B728** (2014) 105–113, [[arXiv:1308.3851](#)].
- [26] L. Bian, T. Li, J. Shu, and X.-C. Wang, *Two component dark matter with multi-Higgs portals*, *JHEP* **03** (2015) 126, [[arXiv:1412.5443](#)].
- [27] S. Esch, M. Klasen, and C. E. Yaguna, *A minimal model for two-component dark matter*, *JHEP* **09** (2014) 108, [[arXiv:1406.0617](#)].
- [28] A. Karam and K. Tamvakis, *Dark matter and neutrino masses from a scale-invariant multi-Higgs portal*, *Phys. Rev.* **D92** (2015), no. 7 075010, [[arXiv:1508.03031](#)].

- [29] A. Karam and K. Tamvakis, *Dark Matter from a Classically Scale-Invariant $SU(3)_X$* , *Phys. Rev. D* **D94** (2016), no. 5 055004, [[arXiv:1607.01001](#)].
- [30] A. DiFranzo and G. Mohlabeng, *Multi-component Dark Matter through a Radiative Higgs Portal*, *JHEP* **01** (2017) 080, [[arXiv:1610.07606](#)].
- [31] S. Bhattacharya, P. Poulose, and P. Ghosh, *Multipartite Interacting Scalar Dark Matter in the light of updated LUX data*, *JCAP* **1704** (2017), no. 04 043, [[arXiv:1607.08461](#)].
- [32] A. Dutta Banik, M. Pandey, D. Majumdar, and A. Biswas, *Two component WIMP-FIMP dark matter model with singlet fermion, scalar and pseudo scalar*, *Eur. Phys. J. C* **C77** (2017), no. 10 657, [[arXiv:1612.08621](#)].
- [33] M. Klasen, F. Lyonnet, and F. S. Queiroz, *NLO+NLL collider bounds, Dirac fermion and scalar dark matter in the $B\ell$ model*, *Eur. Phys. J. C* **C77** (2017), no. 5 348, [[arXiv:1607.06468](#)].
- [34] P. Ghosh, A. K. Saha, and A. Sil, *Study of Electroweak Vacuum Stability from Extended Higgs Portal of Dark Matter and Neutrinos*, *Phys. Rev. D* **D97** (2018), no. 7 075034, [[arXiv:1706.04931](#)].
- [35] A. Ahmed, M. Duch, B. Grzadkowski, and M. Iglicki, *Multi-Component Dark Matter: the vector and fermion case*, [arXiv:1710.01853](#).
- [36] S. Bhattacharya, P. Ghosh, T. N. Maity, and T. S. Ray, *Mitigating Direct Detection Bounds in Non-minimal Higgs Portal Scalar Dark Matter Models*, *JHEP* **10** (2017) 088, [[arXiv:1706.04699](#)].
- [37] D. Borah and A. Dasgupta, *Left Right Symmetric Models with a Mixture of keV-TeV Dark Matter*, [arXiv:1710.06170](#).
- [38] S. Bhattacharya, A. K. Saha, A. Sil, and J. Wudka, *Dark Matter as a remnant of SQCD Inflation*, *JHEP* **10** (2018) 124, [[arXiv:1805.03621](#)].
- [39] S. Bhattacharya, P. Ghosh, and N. Sahu, *Multipartite Dark Matter with Scalars, Fermions and signatures at LHC*, *JHEP* **02** (2019) 059, [[arXiv:1809.07474](#)].
- [40] M. Aoki and T. Toma, *Boosted Self-interacting Dark Matter in a Multi-component Dark Matter Model*, *JCAP* **1810** (2018), no. 10 020, [[arXiv:1806.09154](#)].
- [41] A. Dutta Banik, A. K. Saha, and A. Sil, *Scalar assisted singlet doublet fermion dark matter model and electroweak vacuum stability*, *Phys. Rev. D* **D98** (2018), no. 7 075013, [[arXiv:1806.08080](#)].

- [42] B. Barman, S. Bhattacharya, and M. Zakeri, *Multipartite Dark Matter in $SU(2)_N$ extension of Standard Model and signatures at the LHC*, *JCAP* **1809** (2018), no. 09 023, [[arXiv:1806.01129](#)].
- [43] S. Yaser Ayazi and A. Mohamadnejad, *Scale-Invariant Two Component Dark Matter*, *Eur. Phys. J.* **C79** (2019), no. 2 140, [[arXiv:1808.08706](#)].
- [44] A. Poulin and S. Godfrey, *Multi-component dark matter from a hidden gauged $SU(3)$* , [arXiv:1808.04901](#).
- [45] S. Chakraborti and P. Poulose, *Interplay of Scalar and Fermionic Components in a Multi-component Dark Matter Scenario*, [arXiv:1808.01979](#).
- [46] S. Chakraborti, A. Dutta Banik, and R. Islam, *Probing Multicomponent Extension of Inert Doublet Model with a Vector Dark Matter*, [arXiv:1810.05595](#).
- [47] N. Bernal, D. Restrepo, C. Yaguna, and O. Zapata, *Two-component dark matter and a massless neutrino in a new $B - L$ model*, [arXiv:1808.03352](#).
- [48] F. Elahi and S. Khatibi, *Multi-Component Dark Matter in a Non-Abelian Dark Sector*, [arXiv:1902.04384](#).
- [49] D. Borah, A. Dasgupta, and S. K. Kang, *Two-component Dark Matter with co-genesis of Baryon Asymmetry of the Universe*, [arXiv:1903.10516](#).
- [50] D. Borah, R. Roshan, and A. Sil, *Minimal Two-component Scalar Doublet Dark Matter with Radiative Neutrino Mass*, [arXiv:1904.04837](#).
- [51] S. Bhattacharya, P. Ghosh, A. K. Saha, and A. Sil, *Two component dark matter with inert Higgs doublet: neutrino mass, high scale validity and collider searches*, [arXiv:1905.12583](#).
- [52] S. Profumo, K. Sigurdson, and L. Ubaldi, *Can we discover multi-component WIMP dark matter?*, *JCAP* **0912** (2009) 016, [[arXiv:0907.4374](#)].
- [53] H. Fukuoka, D. Suematsu, and T. Toma, *Signals of dark matter in a supersymmetric two dark matter model*, *JCAP* **1107** (2011) 001, [[arXiv:1012.4007](#)].
- [54] M. Cirelli and J. M. Cline, *Can multistate dark matter annihilation explain the high-energy cosmic ray lepton anomalies?*, *Phys. Rev.* **D82** (2010) 023503, [[arXiv:1005.1779](#)].
- [55] M. Aoki, M. Duerr, J. Kubo, and H. Takano, *Multi-Component Dark Matter Systems and Their Observation Prospects*, *Phys. Rev.* **D86** (2012) 076015, [[arXiv:1207.3318](#)].
- [56] M. Aoki, J. Kubo, and H. Takano, *Two-loop radiative seesaw mechanism with multicomponent dark matter explaining the possible ? excess in the Higgs boson decay and at*

- the Fermi LAT*, *Phys. Rev.* **D87** (2013), no. 11 116001, [[arXiv:1302.3936](#)].
- [57] K. P. Modak, D. Majumdar, and S. Rakshit, *A Possible Explanation of Low Energy γ -ray Excess from Galactic Centre and Fermi Bubble by a Dark Matter Model with Two Real Scalars*, *JCAP* **1503** (2015) 011, [[arXiv:1312.7488](#)].
 - [58] C.-Q. Geng, D. Huang, and L.-H. Tsai, *Imprint of multicomponent dark matter on AMS-02*, *Phys. Rev.* **D89** (2014), no. 5 055021, [[arXiv:1312.0366](#)].
 - [59] P.-H. Gu, *Multi-component dark matter with magnetic moments for Fermi-LAT gamma-ray line*, *Phys. Dark Univ.* **2** (2013) 35–40, [[arXiv:1301.4368](#)].
 - [60] M. Aoki, J. Kubo, and H. Takano, *Multicomponent Dark Matter in Radiative Seesaw Model and Monochromatic Neutrino Flux*, *Phys. Rev.* **D90** (2014), no. 7 076011, [[arXiv:1408.1853](#)].
 - [61] C.-Q. Geng, D. Huang, and L.-H. Tsai, *Cosmic Ray Excesses from Multi-component Dark Matter Decays*, *Mod. Phys. Lett.* **A29** (2014), no. 37 1440003, [[arXiv:1405.7759](#)].
 - [62] C.-Q. Geng, D. Huang, and C. Lai, *Revisiting multicomponent dark matter with new AMS-02 data*, *Phys. Rev.* **D91** (2015), no. 9 095006, [[arXiv:1411.4450](#)].
 - [63] A. Biswas, D. Majumdar, and P. Roy, *Nonthermal two component dark matter model for Fermi-LAT γ -ray excess and 3.55 keV X-ray line*, *JHEP* **04** (2015) 065, [[arXiv:1501.02666](#)].
 - [64] D. Borah, A. Dasgupta, and R. Adhikari, *Common origin of the 3.55 keV x-ray line and the Galactic Center gamma-ray excess in a radiative neutrino mass model*, *Phys. Rev.* **D92** (2015), no. 7 075005, [[arXiv:1503.06130](#)].
 - [65] D. Borah, A. Dasgupta, and S. Patra, *Common origin of 3.55 keV x-ray line and gauge coupling unification with left-right dark matter*, *Phys. Rev.* **D96** (2017), no. 11 115019, [[arXiv:1604.01929](#)].
 - [66] D. Borah, A. Dasgupta, U. K. Dey, S. Patra, and G. Tomar, *Multi-component Fermionic Dark Matter and IceCube PeV scale Neutrinos in Left-Right Model with Gauge Unification*, [[arXiv:1704.04138](#)].
 - [67] J. Herrero-Garcia, A. Scaffidi, M. White, and A. G. Williams, *On the direct detection of multi-component dark matter: sensitivity studies and parameter estimation*, *JCAP* **1711** (2017), no. 11 021, [[arXiv:1709.01945](#)].
 - [68] J. Herrero-Garcia, A. Scaffidi, M. White, and A. G. Williams, *Time-dependent rate of multicomponent dark matter: Reproducing the DAMA/LIBRA phase-2 results*, *Phys. Rev.*

- D98** (2018), no. 12 123007, [[arXiv:1804.08437](#)].
- [69] S. Profumo, F. Queiroz, and C. Siqueira, *Has AMS-02 Observed Two-Component Dark Matter?*, [arXiv:1903.07638](#).
 - [70] S. Weinberg, *Baryon and Lepton Nonconserving Processes*, *Phys. Rev. Lett.* **43** (1979) 1566–1570.
 - [71] P. Minkowski, *$\mu \rightarrow e\gamma$ at a Rate of One Out of 10^9 Muon Decays?*, *Phys. Lett.* **67B** (1977) 421–428.
 - [72] M. Gell-Mann, P. Ramond, and R. Slansky, *Complex Spinors and Unified Theories*, *Conf. Proc.* **C790927** (1979) 315–321, [[arXiv:1306.4669](#)].
 - [73] R. N. Mohapatra and G. Senjanovic, *Neutrino Mass and Spontaneous Parity Violation*, *Phys. Rev. Lett.* **44** (1980) 912.
 - [74] J. Schechter and J. W. F. Valle, *Neutrino Masses in $SU(2) \times U(1)$ Theories*, *Phys. Rev.* **D22** (1980) 2227.
 - [75] R. N. Mohapatra and G. Senjanovic, *Neutrino Masses and Mixings in Gauge Models with Spontaneous Parity Violation*, *Phys. Rev.* **D23** (1981) 165.
 - [76] G. Lazarides, Q. Shafi, and C. Wetterich, *Proton Lifetime and Fermion Masses in an $SO(10)$ Model*, *Nucl. Phys.* **B181** (1981) 287–300.
 - [77] C. Wetterich, *Neutrino Masses and the Scale of B-L Violation*, *Nucl. Phys.* **B187** (1981) 343–375.
 - [78] J. Schechter and J. W. F. Valle, *Neutrino Decay and Spontaneous Violation of Lepton Number*, *Phys. Rev.* **D25** (1982) 774.
 - [79] B. Brahmachari and R. N. Mohapatra, *Unified explanation of the solar and atmospheric neutrino puzzles in a minimal supersymmetric $SO(10)$ model*, *Phys. Rev.* **D58** (1998) 015001, [[hep-ph/9710371](#)].
 - [80] R. Foot, H. Lew, X. G. He, and G. C. Joshi, *Seesaw Neutrino Masses Induced by a Triplet of Leptons*, *Z. Phys.* **C44** (1989) 441.
 - [81] Y. Cai, T. Han, T. Li, and R. Ruiz, *Lepton Number Violation: Seesaw Models and Their Collider Tests*, *Front.in Phys.* **6** (2018) 40, [[arXiv:1711.02180](#)].
 - [82] E. Ma, *Verifiable radiative seesaw mechanism of neutrino mass and dark matter*, *Phys. Rev.* **D73** (2006) 077301, [[hep-ph/0601225](#)].
 - [83] M. Aoki, D. Kaneko, and J. Kubo, *Multicomponent Dark Matter in Radiative Seesaw*

- Models*, *Front.in Phys.* **5** (2017) 53, [[arXiv:1711.03765](#)].
- [84] J. Ellis, M. Fairbairn, and P. Tunney, *Anomaly-Free Dark Matter Models are not so Simple*, *JHEP* **08** (2017) 053, [[arXiv:1704.03850](#)].
 - [85] P. Fileviez Páez, E. Golias, R.-H. Li, C. Murgui, and A. D. Plascencia, *On Anomaly-Free Dark Matter Models*, [arXiv:1904.01017](#).
 - [86] S. F. King, *Littlest Seesaw*, *JHEP* **02** (2016) 085, [[arXiv:1512.07531](#)].
 - [87] R. N. Mohapatra and R. E. Marshak, *Local B-L Symmetry of Electroweak Interactions, Majorana Neutrinos and Neutron Oscillations*, *Phys. Rev. Lett.* **44** (1980) 1316–1319. [Erratum: *Phys. Rev. Lett.* 44,1643(1980)].
 - [88] R. E. Marshak and R. N. Mohapatra, *Quark - Lepton Symmetry and B-L as the U(1) Generator of the Electroweak Symmetry Group*, *Phys. Lett.* **91B** (1980) 222–224.
 - [89] A. Masiero, J. F. Nieves, and T. Yanagida, *$B-l$ Violating Proton Decay and Late Cosmological Baryon Production*, *Phys. Lett.* **116B** (1982) 11–15.
 - [90] R. N. Mohapatra and G. Senjanovic, *Spontaneous Breaking of Global $B-l$ Symmetry and Matter - Antimatter Oscillations in Grand Unified Theories*, *Phys. Rev.* **D27** (1983) 254.
 - [91] W. Buchmuller, C. Greub, and P. Minkowski, *Neutrino masses, neutral vector bosons and the scale of B-L breaking*, *Phys. Lett.* **B267** (1991) 395–399.
 - [92] J. C. Montero and V. Pleitez, *Gauging U(1) symmetries and the number of right-handed neutrinos*, *Phys. Lett.* **B675** (2009) 64–68, [[arXiv:0706.0473](#)].
 - [93] E. Ma and R. Srivastava, *Dirac or inverse seesaw neutrino masses with $B - L$ gauge symmetry and S_3 flavor symmetry*, *Phys. Lett.* **B741** (2015) 217–222, [[arXiv:1411.5042](#)].
 - [94] E. Ma, N. Pollard, R. Srivastava, and M. Zakeri, *Gauge $B - L$ Model with Residual Z_3 Symmetry*, *Phys. Lett.* **B750** (2015) 135–138, [[arXiv:1507.03943](#)].
 - [95] B. L. Sánchez-Vega, J. C. Montero, and E. R. Schmitz, *Complex Scalar DM in a B-L Model*, *Phys. Rev.* **D90** (2014), no. 5 055022, [[arXiv:1404.5973](#)].
 - [96] B. L. Sánchez-Vega and E. R. Schmitz, *Fermionic dark matter and neutrino masses in a B-L model*, *Phys. Rev.* **D92** (2015) 053007, [[arXiv:1505.03595](#)].
 - [97] S. Singirala, R. Mohanta, and S. Patra, *Singlet scalar Dark matter in $U(1)_{B-L}$ models without right-handed neutrinos*, [arXiv:1704.01107](#).
 - [98] T. Nomura and H. Okada, *Radiative neutrino mass in an alternative $U(1)_{B-L}$ gauge symmetry*, [arXiv:1705.08309](#).

- [99] W. Wang and Z.-L. Han, *Radiative linear seesaw model, dark matter, and $U(1)_{B-L}$* , *Phys. Rev. D* **92** (2015) 095001, [[arXiv:1508.00706](#)].
- [100] S. Patra, W. Rodejohann, and C. E. Yaguna, *A new $B \rightarrow L$ model without right-handed neutrinos*, *JHEP* **09** (2016) 076, [[arXiv:1607.04029](#)].
- [101] A. Biswas and A. Gupta, *Calculation of Momentum Distribution Function of a Non-thermal Fermionic Dark Matter*, *JCAP* **1703** (2017), no. 03 033, [[arXiv:1612.02793](#)]. [Addendum: JCAP1705,no.05,A02(2017)].
- [102] D. Nanda and D. Borah, *Common origin of neutrino mass and dark matter from anomaly cancellation requirements of a $U(1)_{B-L}$ model*, *Phys. Rev. D* **96** (2017), no. 11 115014, [[arXiv:1709.08417](#)].
- [103] A. Biswas, D. Borah, and D. Nanda, *When Freeze-out Precedes Freeze-in: Sub-TeV Fermion Triplet Dark Matter with Radiative Neutrino Mass*, *JCAP* **1809** (2018), no. 09 014, [[arXiv:1806.01876](#)].
- [104] M. Carena, A. Daleo, B. A. Dobrescu, and T. M. P. Tait, *Z' gauge bosons at the Tevatron*, *Phys. Rev. D* **70** (2004) 093009, [[hep-ph/0408098](#)].
- [105] G. Cacciapaglia, C. Csaki, G. Marandella, and A. Strumia, *The Minimal Set of Electroweak Precision Parameters*, *Phys. Rev. D* **74** (2006) 033011, [[hep-ph/0604111](#)].
- [106] **ATLAS** Collaboration, M. Aaboud et al., *Search for new high-mass phenomena in the dilepton final state using 36.1 fb^{-1} of proton-proton collision data at $\sqrt{s} = 13 \text{ TeV}$ with the ATLAS detector*, [arXiv:1707.02424](#).
- [107] **ATLAS** Collaboration, G. Aad et al., *Search for high-mass dilepton resonances using 139 fb^{-1} of pp collision data collected at $\sqrt{s} = 13 \text{ TeV}$ with the ATLAS detector*, *Phys. Lett. B* **796** (2019) 68–87, [[arXiv:1903.06248](#)].
- [108] **CMS** Collaboration, A. M. Sirunyan et al., *Search for high-mass resonances in dilepton final states in proton-proton collisions at $\sqrt{s} = 13 \text{ TeV}$* , *JHEP* **06** (2018) 120, [[arXiv:1803.06292](#)].
- [109] B. Barman, D. Borah, P. Ghosh, and A. K. Saha, *Flavoured gauge extension of singlet-doublet fermionic dark matter: neutrino mass, high scale validity and collider signatures*, [arXiv:1907.10071](#).
- [110] T. Robens and T. Stefaniak, *Status of the Higgs Singlet Extension of the Standard Model after LHC Run 1*, *Eur. Phys. J. C* **75** (2015) 104, [[arXiv:1501.02234](#)].

- [111] G. Chalons, D. Lopez-Val, T. Robens, and T. Stefaniak, *The Higgs singlet extension at LHC Run 2, PoS ICHEP2016* (2016) 1180, [[arXiv:1611.03007](#)].
- [112] D. L  pez-Val and T. Robens, *$\tilde{I}\tilde{T}r$ and the W -boson mass in the singlet extension of the standard model*, *Phys. Rev.* **D90** (2014) 114018, [[arXiv:1406.1043](#)].
- [113] **CMS** Collaboration, V. Khachatryan et al., *Search for a Higgs boson in the mass range from 145 to 1000 GeV decaying to a pair of W or Z bosons*, *JHEP* **10** (2015) 144, [[arXiv:1504.00936](#)].
- [114] M. J. Strassler and K. M. Zurek, *Discovering the Higgs through highly-displaced vertices*, *Phys. Lett.* **B661** (2008) 263–267, [[hep-ph/0605193](#)].
- [115] G. Belanger and J.-C. Park, *Assisted freeze-out*, *JCAP* **1203** (2012) 038, [[arXiv:1112.4491](#)].
- [116] A. Biswas, *Explaining Low Energy γ -ray Excess from the Galactic Centre using a Two Component Dark Matter Model*, *J. Phys.* **G43** (2016), no. 5 055201, [[arXiv:1412.1663](#)].
- [117] P. Gondolo and G. Gelmini, *Cosmic abundances of stable particles: Improved analysis*, *Nucl. Phys.* **B360** (1991) 145–179.
- [118] G. B  llanger, F. Boudjema, A. Pukhov, and A. Semenov, *micrOMEGAs4.1: two dark matter candidates*, *Comput. Phys. Commun.* **192** (2015) 322–329, [[arXiv:1407.6129](#)].
- [119] A. Alloul, N. D. Christensen, C. Degrande, C. Duhr, and B. Fuks, *FeynRules 2.0 - A complete toolbox for tree-level phenomenology*, *Comput. Phys. Commun.* **185** (2014) 2250–2300, [[arXiv:1310.1921](#)].
- [120] A. Belyaev, N. D. Christensen, and A. Pukhov, *CalcHEP 3.4 for collider physics within and beyond the Standard Model*, *Comput. Phys. Commun.* **184** (2013) 1729–1769, [[arXiv:1207.6082](#)].
- [121] A. Berlin, D. Hooper, and S. D. McDermott, *Simplified Dark Matter Models for the Galactic Center Gamma-Ray Excess*, *Phys. Rev.* **D89** (2014), no. 11 115022, [[arXiv:1404.0022](#)].
- [122] M. Cirelli, N. Fornengo, and A. Strumia, *Minimal dark matter*, *Nucl. Phys.* **B753** (2006) 178–194, [[hep-ph/0512090](#)].
- [123] E. Ma and D. Suematsu, *Fermion Triplet Dark Matter and Radiative Neutrino Mass*, *Mod. Phys. Lett.* **A24** (2009) 583–589, [[arXiv:0809.0942](#)].
- [124] **ATLAS** Collaboration, M. Aaboud et al., *Search for long-lived charginos based on a disappearing-track signature in pp collisions at $\sqrt{s} = 13$ TeV with the ATLAS detector*, *JHEP* **06** (2018) 022, [[arXiv:1712.02118](#)].

- [125] D. Curtin et al., *Long-Lived Particles at the Energy Frontier: The MATHUSLA Physics Case*, [arXiv:1806.07396](#).